TRANSPORTATION RESEARCH RECORD 788

Interaction Between Vehicles and Pavement Surfaces

TRANSPORTATION RESEARCH BOARD

COMMISSION ON SOCIOTECHNICAL SYSTEMS
NATIONAL RESEARCH COUNCIL

NATIONAL ACADEMY OF SCIENCES
WASHINGTON, D.C. 1980

Transportation Research Record 788
Price $4.20
Edited for TRB by Naomi Kassabian

modes
1 highway transportation
4 air transportation

subject area
24 pavement design and performance

Library of Congress Cataloging in Publication Data
National Research Council. Transportation Research Board.
Interaction between vehicles and pavement surfaces.

(Transportation research record; 788)
Reports presented at the 59th annual meeting of the Transportation Research Board.
1. Automobiles–Skidding–Addresses, essays, lectures. 2. Pavements–Addresses, essays, lectures. I. National Research Council (U.S.). Transportation Research Board. II. Series.
TE7.H5 no. 788 [TL295] 380.5s [625.8] 81-9589
ISBN 0-309-03202-4 ISSN 0361-1981 AACR2

Sponsorship of the Papers in This Transportation Research Record

GROUP 2–DESIGN AND CONSTRUCTION OF TRANSPORTATION FACILITIES
R. V. LeClerc, Washington State Department of Transportation, chairman

Pavement Design Section
W. Ronald Hudson, University of Texas at Austin, chairman

Committee on Surface Properties–Vehicle Interaction
Don L. Ivey, Texas A&M University, chairman
Glenn G. Balmer, Frederick E. Behn, Robert R. Blackburn, John C. Burns, A. Y. Casanova III, John D. Eagleburger, Robert D. Ervin, Carlton M. Hayden, Rudolph R. Hegmon, Edward D. Howerter, Kenneth J. Law, David C. Mahone, W. E. Meyer, Thomas H. Morrow, Jr., W. Grigg Mullen, Bobby G. Page, A. Scott Parrish, Bayard E. Quinn, John J. Quinn, J. Reichert, Hollis B. Rushing, Elson B. Spangler, James C. Wambold, E. A. Whitehurst

Lawrence F. Spaine, Transportation Research Board staff

The organizational units, officers, and members are as of December 31, 1979.

Contents

Authors of the Papers in This Record

Agrawal, S.K., Federal Aviation Administration, Technical Center, ANA-4A, Building 14, Atlantic City, NJ 08405
Balmer, G.G., Federal Highway Administration, U.S. Department of Transportation, 400 Seventh Street, S.W., Washington, DC 20590
Burchett, James L., Kentucky Department of Transportation, 533 South Limestone Street, Lexington, KY 40508
Hegmon, R.R., Federal Highway Administration, U.S. Department of Transportation, 400 Seventh Street, S.W., Washington, DC 20590
Heinsohn, Robert J., Pennsylvania State University, Research Building B, University Park, PA 16802
Henry, John Jewett, Pennsylvania State University, Research Building B, University Park, PA 16802
Rizenbergs, R.L., Kentucky Department of Transportation, 533 South Limestone Street, Lexington, KY 40508
Shakely, Roger B., Pennsylvania State University, Research Building B, University Park, PA 16802

Use of Blank and Ribbed Test Tires for Evaluating Wet-Pavement Friction

JOHN JEWETT HENRY

Skid-resistance data are compared by the ASTM E274 locked-wheel test method that uses blank E524 and ribbed E501 test tires on 59 pavements. The ribbed E501 tire is shown to be a poor discriminator of the drainage capability from the tire-pavement interface produced by pavement macrotexture. The blank E524 test tire is shown to produce data sensitive to both macrotexture and microtexture. The pavements included in the study range from well-polished and worn dense-graded asphalt and portland cement concrete to open-graded asphalt grooved portland cement concrete; they ranged in SN_{40} from 24 to 69 with the ribbed tire. It is also noted that the ribbed E501 tire provides better drainage than do most passenger car tires during the latter third of their usable life.

Wet-pavement friction of the primary highway systems of most states is monitored in annual surveys by using the full-scale locked-wheel skid-test procedure specified by ASTM E274. The skid resistance is reported as a skid number (SN), which is the friction force as a percentage of the vertical load for a test tire that is sliding at the speed of the test, usually 65 km/h (40 miles/h). The application of water to the pavement, range of vertical load, operating conditions, and all other details specified by the procedure are implied when pavement friction is reported by SNs. Also implied is the use of the ASTM ribbed test tire specified by ASTM E501.

The E501 tire has seven circumferential ribs that form six grooves to provide for drainage of water from the tire-pavement interface as the tire slides over the wet pavement during a test. The specification requires that the tire not be reused when the minimum depth of the grooves reaches 4 mm (0.16 in). The use of excessively worn test tires produces lower SNs. Figures 1 and 2 show a conceptualized ribbed test tire on actual profiles of dense-graded and open-graded asphalt concrete pavement (ACP). The scale is distorted by the differences in vertical and horizontal magnifications (vertical = 8X; horizontal = 1.5X for both pavement profile and tire). From these figures it can be seen that the tire contributes a significant amount of the drainage area. Furthermore, the drainage area provided by the tire grooves is continuous and unimpeded in the longitudinal direction, unlike that provided by the pavement.

It is an accepted procedure to rehabilitate portland cement concrete (PCC) pavement by sawing longitudinal grooves into the surface. It has been noted (1,2) that the SN is not significantly improved by grooving. Figure 3 shows the profile of the ribbed test tire superimposed on a typical grooving pattern [6.4x4-mm grooves on 25-mm spacing (0.25x0.25-in grooves on 1-in spacing)]; the figure is scaled with the same magnification as in Figures 1 and 2 for comparison. Since the presence or absence of the grooves does not affect the SN, it is apparent that sufficient drainage is provided by the tire grooves. If the SN were a true measure of the safety, grooving of PCC pavements could not be justified.

Passenger car tires have tread patterns that provide varying amounts of drainage area. Ink-impression prints of a passenger car tire when new and when worn were made, and the mean effective tread depth (open area divided by total area times mean tread depth) was computed. A comparison of mean effective tread depth measured for passenger car tires and the E501 ribbed test tire is given below (1 mm = 0.04 in):

Tire	Minimal Tread Depth (mm)	Mean Effective Tread Depth (mm)
Passenger car		
New	10.4	1.98
Worn (legal limit)	2.4	0.41
E501		
New	9.5	2.01
Worn	4.0	0.97

Although the new test tire and passenger car tire have the same drainage capabilities, their worn counterparts do not. The worn test tire has approximately one-half the mean effective tread depth of the new test tire. For more than one-third of its useful life, the passenger car tire has less mean effective tread depth than the completely worn test tire if one assumes that the tread wears linearly with time. It also should be noted that the passenger car tire used here has an above-average tread depth.

Attempts to relate wet-weather accident frequency to SNs have not been encouraging. The most extensive studies, conducted in Kentucky (3,4), suggest a trend, but the scatter is large and the correlation coefficients are low. A conclusion that might be drawn is that actual tires depend to a greater extent on the contribution of pavement texture to drainage than does the ribbed test tire. Conversely, it could be stated that testing by using the ribbed tire is not sufficiently sensitive to the pavement texture that actual tires depend on for prevention of wet skidding.

ROLE OF PAVEMENT TEXTURE

The two scales of pavement texture of significance to wet-pavement friction are microtexture, which has a space frequency content of more than 2000 cycles/m (50 cycles/in), and macrotexture, which has a space frequency range from 25 to 2000 cycles/m (0.65-50 cycles/in) (5). Microtexture influences the general level of the SN, whereas macrotexture determines the rate of decrease of skid resistance with speed. SN data are shown (5) to decrease experimentally with speed according to the following model:

$$SN = SN_0 \exp[-(PNG/100)v] \quad (1)$$

where, for ribbed-tire data, SN_0 is found to be linearly related to measures of microtexture, whereas PNG is inversely related to the square root of macrotexture parameters. The parameter SN_0 also has the significance of being the zero-speed intercept of fit to the SN data and PNG is the percent normalized gradient, related to the SN and SN-speed gradient (SNG) as follows:

$$PNG = (SNG/SN) \times 100 = (-100/SN)(dSN/dV) \quad (2)$$

The low-speed or zero-speed friction indicated by the value of SN_0 increases with such microtexture

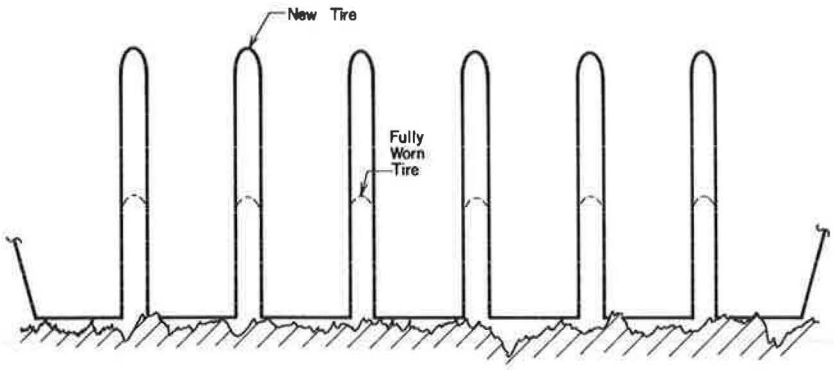

Figure 1. ASTM ribbed test tire on dense-graded ACP.

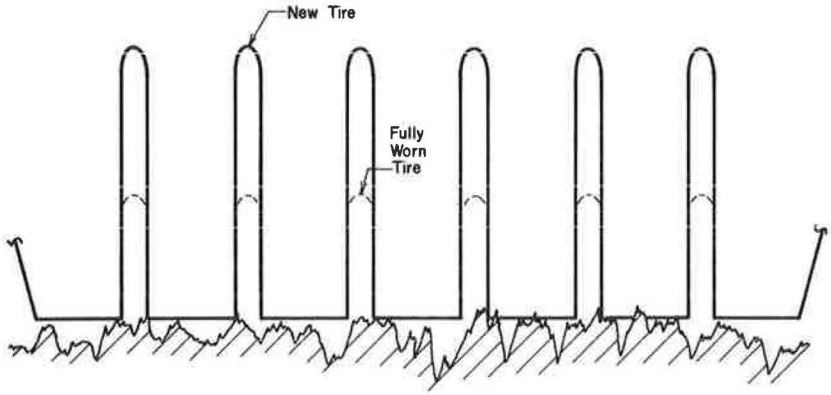

Figure 2. ASTM ribbed test tire on open-graded ACP.

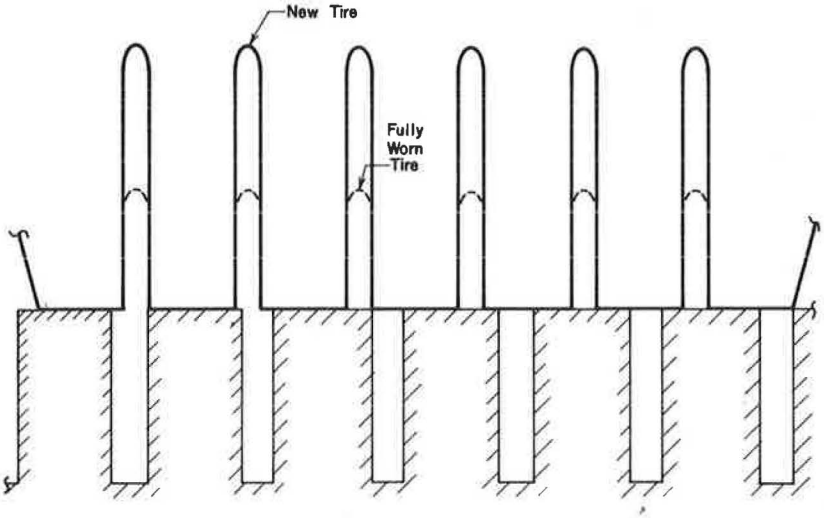

Figure 3. ASTM ribbed test tire on grooved PCC pavement.

parameters as height of the microtexture profile and British pendulum number (BPN). The rate at which the SN decreases with speed decreases with increasing macrotexture parameters such as the height of the macrotexture profiles and sandpatch mean texture depth. Good skid resistance at traffic speeds such as 65 km/h (40 miles/h) requires high levels of both macrotexture and microtexture. The comparisons of the drainage capabilities provided by the test tire and a passenger car tire given in the previous section and the drainage provided by the pavement macrotexture led to the question whether the ribbed tire has sufficient sensitivity to the macrotexture.

BLANK TEST TIRE

The blank test tire specified by ASTM E524 is, except for the absence of the grooves, the same as the E501 ribbed tire. Clearly, its contribution to drainage capability from the tire-pavement interface is zero, and one would therefore expect it to produce data that have a strong dependence on macrotexture for measurements at 65 km/h. The blank tire is an extreme case; actual tires rank between it and the ribbed tire in drainage capability. However, an intermediate test tire--for example, one with shallower grooves--would be impractical, since it would have a very limited useful life. That is, either the grooves must be sufficiently deep so that their

Figure 4. Effects of water-flow rate on skid-resistance measurements (Pennsylvania State nozzle).

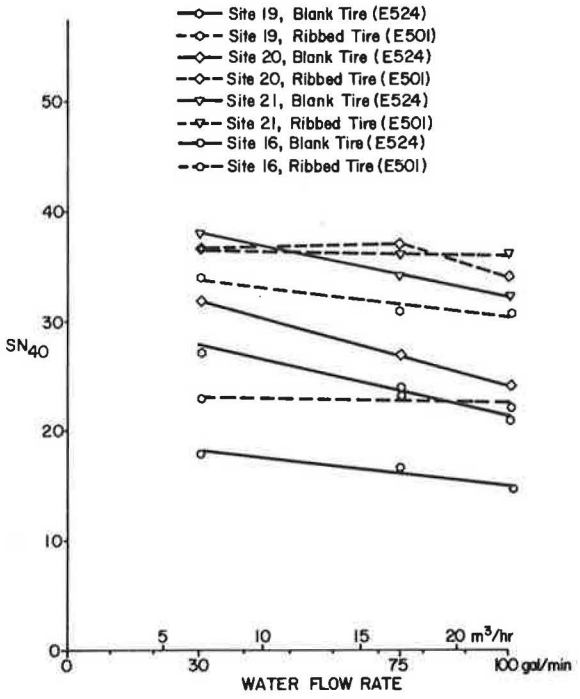

Figure 5. Blank- and ribbed-tire test data on PCC pavement.

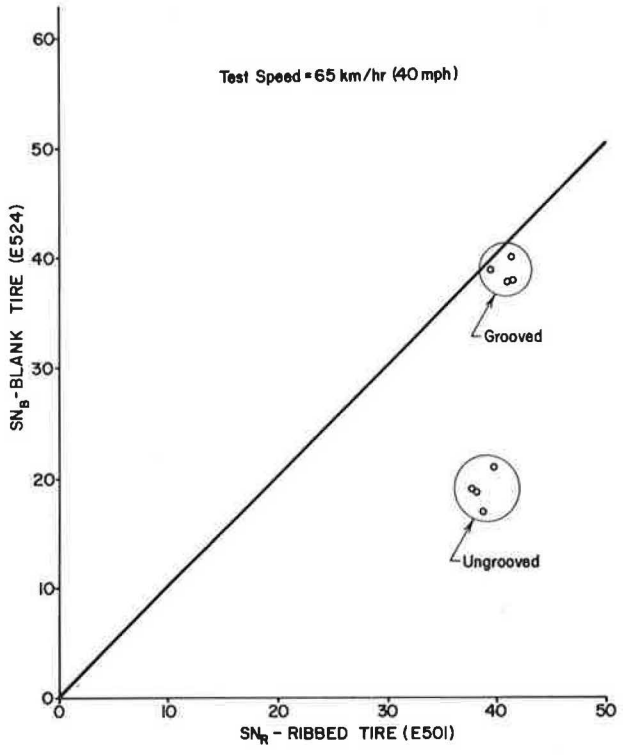

depth does not affect the test or they must be absent.

It has been suggested that a disadvantage of the blank tire is that it also is sensitive to the amount of water on the pavement. ASTM E274 specifies water-flow rates that would produce a water-film thickness of 0.5 mm (0.020 in) if all the water were to lie uniformly on the pavement in the tire path. Actual film thicknesses are undoubtedly somewhat less. The ribbed test tire, which has a terminal mean effective tread depth of 0.97 mm (0.038 in), can easily permit the escape of this amount of water or more without a noticeable decrease in friction. Tests were run by using both tires over four pavements and water flow from 6.8 to 22.7 m^3/h (30-100 gal/min); the results are shown in Figure 4. Although the effect of the rate of water delivery to the test tire is pronounced for the blank tire, there is no severe problem if reasonable calibration of the water-flow rate is maintained. At 65 km/h the ribbed tire can accept as much as three times the normal water-flow rate without the data being affected by more than three SNs. The fact that it is insensitive to water-flow rate casts doubt on the validity of the ribbed tire as a means of evaluating pavements for wet-weather safety. It is, however, convenient in that the data are not affected seriously by variations in water delivery caused by poorly calibrated watering systems.

COMPARISON OF SKID TESTING BETWEEN BLANK AND RIBBED TEST TIRES

Data are available from tests that used both the blank and ribbed tires for skid-test programs in Pennsylvania and in Virginia. Early interest in the blank tire for evaluating grooved PCC pavements prompted tests on grooved and ungrooved sections of an Interstate highway (2). All tests were conducted at 65 km/h according to ASTM E274 with the exception that the E524 tire was used for blank-tire testing and is reported as SN_B. All testing was performed on the same day on four sets of grooved and ungrooved pavements. The data are presented below and plotted in Figure 5 (2).

	Grooved		Ungrooved	
Test Site	SN_B	SN_R	SN_B	SN_R
A	38	42	19	38
B	40	42	17	39
C	39	40	19	38
D	38	42	21	40

The measurements indicate a distinct improvement in SN_B as a result of grooving. In fact, there is only a small difference between SN_B and the ribbed-tire data (SN_R) on the grooved sections, which indicates that there is adequate macrotexture in the pavement to provide for drainage.

On the ungrooved sections, the ribbed tire provides adequate drainage and can barely distinguish ungrooved from grooved sections, whereas the blank-tire data clearly demonstrate the lack of macrotexture.

A study in Virginia that used both tires (6) indicates similar results with a wide variety of pavement types, including special surface treatments, tined surfaces, and open-graded and conventional pavements. The data from this study are plotted in Figure 6. Three groups of data are indicated on Figure 6--surfaces described in the text as having "good macrotexture," as having average macrotexture, and as being "smooth." Surfaces on which the pavement provides good drainage lie close to or above the line of equality. The blank tire ranks the pavement into groups according to the qualitative descriptions of their texture.

At Pennsylvania State University in the fall of 1978 and spring of 1979, 22 sites were tested with both tires. Sandpatch data [mean texture depth (MTD) according to the Portland Cement Association method (7)] and British pendulum tests (BPN

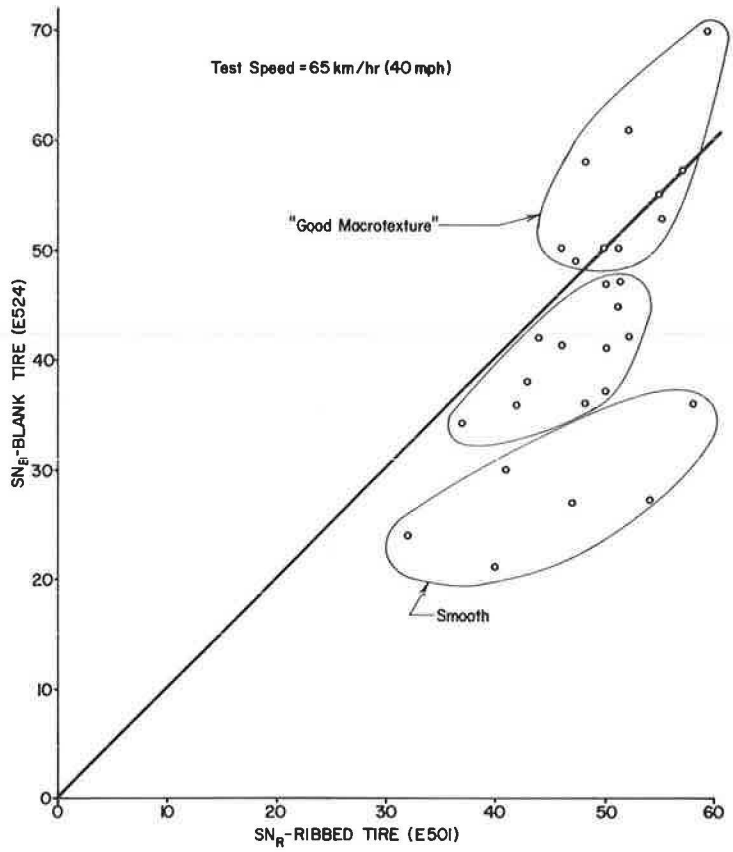

Figure 6. Data from Virginia study by Mahone.

Table 1. Pennsylvania State University data.

Site Characteristics				Fall 1978				Spring 1979			
No.	Year Constructed	Type[a]	ADT	SN_B	SN_R	MTD (milli-in)	BPN	SN_B	SN_R	MTD (milli-in)	BPN
1	1970	DG	6630	22.8	32.4	16	50.7	22.7	31.7	14	46.3
2	1950	PCC	7700	19.0	28.2	14	59.0	14.7	27.4	16	51.7
3	1973	PCC	3640	28.4	49.4	13	69.9	19.7	38.0	15	68.1
4	1972	DG	3640	25.6	39.4	12	58.7	23.3	35.0	13	50.1
5	1976	OG	7700	56.0	53.0	51	86.0	-	-	-	-
6	1976	DG	7700	42.5	52.5	22	81.1	-	-	-	-
7	1973	PCC	1820	27.2	48.5	16	70.4	23.4	40.4	15	64.0
8	1972	DG	1820	44.2	46.2	29	59.3	26.7	32.2	28	52.0
9	1972	DG	1710	46.8	52.2	27	66.0	34.6	43.2	31	56.9
10	1973	PCC	1710	26.2	48.4	14	73.0	22.7	43.2	13	70.1
11	1963	DG	4490	21.6	30.2	14	59.9	18.8	27.3	19	47.8
12	1970	DG	4490	34.8	39.8	40	67.7	31.0	40.6	31	57.6
13	1969	OG	7920	61.4	60.0	41	94.2	60.7	64.5	52	88.7
14	1967	PCC	8770	24.8	37.0	16	63.8	21.4	37.9	18	61.1
15	1969	OG	7920	61.1	62.6	51	96.9	62.2	68.6	54	86.6
16	1966	DG	6500	17.8	25.4	26	55.5	14.7	24.1	23	44.1
17	1961	DG	800	33.0	35.8	40	58.0	29.4	35.4	44	50.0
18	1973	PCC	1200	37.8	50.6	20	69.5	34.0	47.6	21	67.0
19	1968	DG	7000	26.6	37.4	17	63.0	19.5	30.3	20	49.1
20[b]	1968	DG	-	37.5	47.5	21	65.0	25.3	33.6	22	57.0
21	1969	OG	2500	36.6	36.2	49	70.0	32.3	36.2	48	53.2
22	1969	OG	2500	61.4	57.6	55	87.5	56.2	60.2	64	87.7
24	1963	DG	4490	-	-	-	-	14.4	26.1	16	46.2
25	1969	OG	7920	-	-	-	-	40.8	53.8	27	76.7

Note: 1 milli-in = 0.025 mm.
[a]PCC = Portland cement concrete; DG = dense-graded asphalt concrete; OG = open-graded asphalt concrete.
[b]Site 20 is between the wheel tracks at site 19.

according to ASTM E303) were obtained. The data from these tests are given in Table 1. The test in the fall of 1978 and the four tests in the spring of 1979 are treated separately, since the winter affected the texture. Also, sites 5 and 6 were replaced by 24 and 25 in 1979 due to the complete failure of site 5 as a result of snow-removal activities. The data are plotted in Figures 7 and 8, in which the site number, MTD, and BPN (rounded) are indicated for each point.

Examination of Figures 7 and 8 shows that the ribbed tire ranks the pavements more strongly according to microtexture (BPN) than does the blank tire. The blank tire, however, ranks both according

Figure 7. Data from Pennsylvania State study, fall 1978.

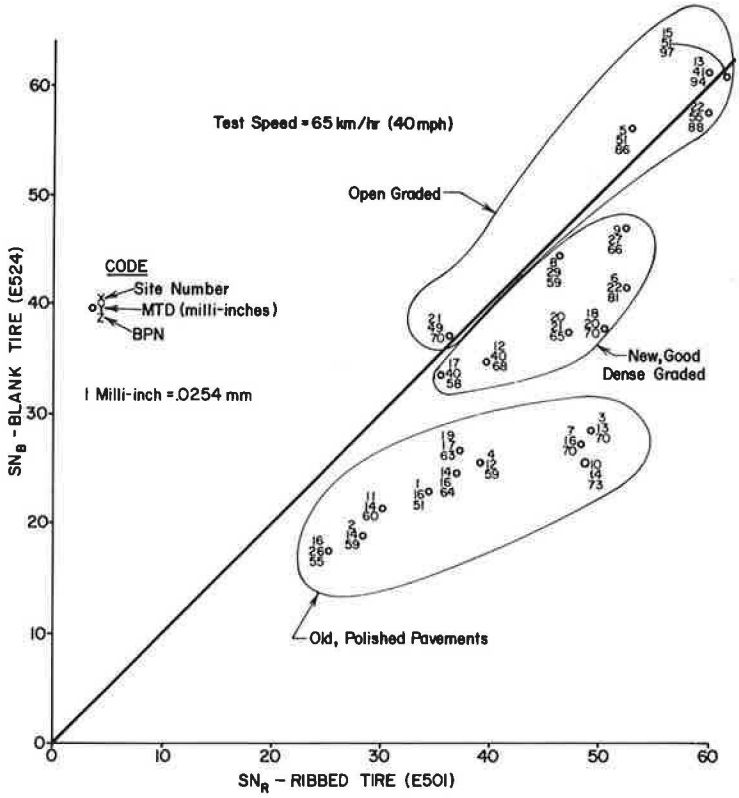

Figure 8. Data from Pennsylvania State study, spring 1979.

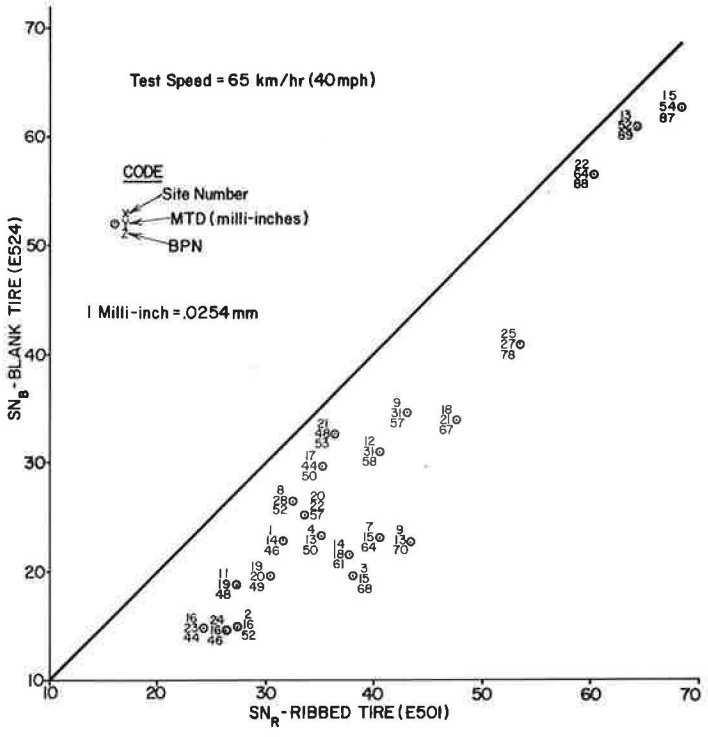

to microtexture (BPN) and macrotexture (MTD), whereas the ribbed tire is unable to distinguish differences in macrotexture.

A multiple linear regression was performed on the data in the following form:

$$SN = a_0 + a_1(BPN) + a_2(MTD) \quad (3)$$

Table 2 shows the results of the regression, which summarizes the coefficients (a_1) and the correlation coefficients (R^2). The values of the coefficients are of interest in evaluating the sensitivity of the test tires to microtexture and macrotexture. The coefficient of macrotexture a_2 is small for the ribbed tire and even has a dif-

Table 2. Correlation of skid numbers with texture data.

Test	Tire Data Type	Coefficient a_0	a_1	a_2	R^2
Fall 1978	SN_B	-19.68	0.64	0.41	0.813
	SN_R	-7.83	0.80	-0.12	0.740
Spring 1979	SN_B	-16.87	0.54	0.50	0.906
	SN_R	-9.19	0.74	0.15	0.926

ferent sign for the two data sets. The coefficients a_1 and a_2 for the blank tire are similar in magnitude, which indicates comparable sensitivity to microtexture and macrotexture.

CONCLUSIONS AND RECOMMENDATIONS

The results of this study indicate that the ribbed E501 test tire provides a good evaluation of microtexture but is not sensitive to macrotexture, which is felt to be a significant factor in wet-pavement safety. This may account for a lack of correlation between skid-resistance measurements by using the ribbed tire and accident statistics.

Ideally, a pavement skid-resistance survey would be performed by using both the ribbed E501 and the blank E524 tires. By comparing the skid-resistance values from both tires, one can readily estimate the levels of microtexture and macrotexture and assess the cause of poor skid resistance and likelihood of success of corrective action.

In the event that skid-resistance surveys can be performed with one tire only, the blank E524 tire appears to be the stronger candidate. At this writing, no attempts to correlate smooth-tire data with accident frequency are known to me, although in one state some data are reportedly being collected. A study to relate blank-tire data to accident frequency should be conducted to verify this conclusion.

Since this research was initiated, the manufacture of the E524 tire has been suspended due to lack of demand. Preliminary tests indicate that a used E501 tire that has the ribs machined away completely and has been subjected to a 350-km (200-mile) break-in produces results that are in excellent agreement with those of the E524 tire. Such a tire will not have a long useful life but will serve as an interim tire for research until demand for the blank tire increases.

REFERENCES

1. R. J. Rasmussen. Pavement Surface Texturing and Restoration for Highway Safety. Presented at the 53rd Annual Meeting, HRB, 1974.
2. V. R. Shah and J. J. Henry. Relationship of Locked-Wheel Friction to That of Other Test Modes. Pennsylvania Department of Transportation, Harrisburg, Final Rept. on Agreement 52489, Feb. 1977.
3. R. L. Rizenbergs, J. L. Burchett, J. A. Deacon, and C. T. Napier. Accidents on Rural Interstate and Parkway Roads and Their Relation to Pavement Friction. TRB, Transportation Research Record 584, 1975, pp. 22-36.
4. R. L. Rizenbergs, J. L. Burchett, and L. Warren. Accidents on Rural, Two-Lane Roads and Their Relation to Pavement Friction. Kentucky Bureau of Highways, Frankfort, Research Rept. 458, 1976.
5. J. J. Henry. The Relationship Between Texture and Pavement Friction. Presented as 1977 Kummer Lecture at ASTM Annual Meeting, St. Louis, MO, Dec. 1977.
6. D. C. Mahone. An Evaluation of the Effects of Tread Depth, Pavement Texture, and Water Film Thickness on Skid Number--Speed Gradients. Virginia Highway and Transportation Research Council; Federal Highway Administration, U.S. Department of Transportation, March 1975.
7. Interim Recommendations for the Construction of Skid-Resistant Concrete Pavement. American Concrete Paving Association, Oak Brook, IL, Tech. Bull. 6, 1969.

Seasonal Variations in the Skid Resistance of Pavements in Kentucky

JAMES L. BURCHETT AND ROLANDS L. RIZENBERGS

Frequent measurements of skid resistance were made on 20 pavements in common use in Kentucky from November 1969 through 1973. Principal analysis involved relating changes in skid resistance to day of the year and relating skid resistance to temperature at the time of test, to average antecedent temperatures, and to average rainfall. Seasonal variations exhibited an annual sinusoidal cycle. The changes in sand-asphalt and bituminous concrete surfaces under high volumes of traffic were about 12 skid numbers (SNs). The changes in portland cement concrete (PCC) and bituminous concrete under low volumes of traffic were about 5 SNs. The lowest SN values occurred in early to mid-August for PCC and sand-asphalt pavements and in late August to early September for bituminous concrete. Correlations between changes in SN and temperature were best for ambient air temperature averaged over four- and eight-week periods prior to date of test. However, correlations between changes in SN and temperature were not so good as correlations between SN and day of the year. On the other hand, combining traffic volumes in the form of deviations from yearly average daily traffic with temperature yielded correlations with SN that were as good as correlations between SN and the day of the year. It was concluded that skid-resistance measurements in Kentucky should be conducted between the first of July and the middle of November to assure detection of significant differences in SN. However, frequent testing of reference sections is recommended to define more specifically each year the beginning and ending dates of the testing season.

Laboratory studies of wear and frictional characteristics of aggregates in Kentucky began in 1956, and field testing of pavement surfaces began in 1958. Many variables associated with testing devices, procedures, and methods of test were investigated and led eventually to standardization. From 1958 to 1969, field tests were conducted with an automobile in several modes (1). Testing then was confined mostly to a six-month period from mid-May through mid-November. Also, the greater

manpower needs for testing with an automobile could best be satisfied in the summer. However, concerns persisted with regard to the influence of weather and the seasonal changes. A limited investigation of seasonal changes was conducted during 1965, 1966, and 1967. Results then indicated significant fluctuations, but the data were insufficient to define the change (2).

A two-wheeled skid-test trailer was acquired in 1969 and was adapted for routine testing (3). Statewide surveys were initiated, and the data were used for a multiplicity of purposes, which included the identification of hazardous locations in wet weather. The test period needed to be defined to minimize variability. Also, measurements outside the test period needed to be adjusted to a common base.

Periodic measurements were initiated in 1969 on 20 pavement sections; there were four types of surfaces. Tests were conducted from November 1969 through 1973. Changes in skid resistance were related to day of the year. Relationships were sought between skid resistance and temperature at the time of test, average temperature for one to eight weeks prior to the day of test, and average rainfall. This paper presents those analyses.

DATA

Pavement Sections

A total of 20 pavement sections was selected that were within 48 km (30 miles) of Lexington. Fourteen were 2.4 km (1.5 miles) long and the other six were 1.6 km (1.0 mile) long. The sections were bituminous (class 1, types A and B), sand-asphalt, and portland cement concrete (PCC). The annual average daily traffic (AADT) per lane ranged from 200 to 10 300. Each section was at least three years old; therefore, polishing effects due to traffic had stabilized.

Weather

Precipitation and temperatures were obtained from monthly Environmental Data Service tabulations of local climatological data for the Lexington area. Average precipitation was determined in terms of both quantity and duration. Average temperatures for periods of one, two, three, four, and eight weeks preceding tests were calculated from daily average temperatures, which were determined by averaging 3-h readings. Monthly average temperatures were recorded. Ambient air temperature and pavement surface temperature were measured and recorded at the time of test.

Skid-Resistance Measurement

Skid resistance was measured with a surface-dynamics pavement friction tester (model 965A) manufactured by K. J. Law Engineers, Incorporated, Detroit, Michigan. The two-wheeled skid-test trailer was acquired in 1969. This trailer complied with ASTM E274-70. The measurements represent the traction developed between a standard 36-mm (14-in) test tire (ASTM E249-66) and a wetted pavement. The locked-wheel measurements are expressed in skid numbers (SNs).

From November 1969 to December 1972, the test sections were tested on a monthly basis. Six of the sections were overlaid in June 1972. Testing continued during March and June 1973 on the 14 remaining sections. Equipment malfunctions, weather conditions, and other circumstances prevented testing during some months. In all, tests were made during two-thirds of the scheduled months.

Measurements were made in the left wheel path at 17.9 m/s (40 miles/h). Tests were also made at 8.9 m/s (20 miles/h) and at 26.8 m/s (60 miles/h) during one-half of the schedule.

SN VERSUS DAY OF YEAR

From the 17.9-m/s tests, the SN was plotted versus date of test. These plots indicated that the SN varies sinusoidally during the year. It was desirable to derive an equation to indicate the day of occurrence of the highest and lowest SN values. Therefore, the model equation for the regression analysis was based on the cosine function; one cycle encompassed 365 days. This equation was as follows:

$$SN_p = SN_a - \Delta SN \cos [360^\circ(D - D_l)/365] \quad (1)$$

where

SN_p = predicted SN,
SN_a = SN about which SN varies,
ΔSN = largest variation of SN about SN_a,
D = day of year, and
D_l = day of year at which SN is lowest.

The values of SN_a, ΔSN, and D_l were determined for each test section by using the method of least squares. These values, along with other statistics, are presented in Table 1. The variations in SN were determined for each section by subtracting SN_a from SN_p. The resulting curves are shown in Figure 1.

The variances in SN on bituminous surfaces were associated with traffic volume. For example, section 1, which has a 16-point change, was the same construction project as section 2, which had only a 12-point change. Section 1, however, was the outer lane and had a higher AADT than did section 2. The same was true for pairs of sections 5 and 6, 7 and 8, 9 and 10, and 17 and 18. All other sections were on two-lane roads and therefore pairs of sections had nearly the same AADT. These pairs were sections 3 and 4, 11 and 12, and 19 and 20. There was very little difference in the SNs in those cases.

Changes in the SN ($SN - SN_a$) for each type of surface were combined, and regression equations were determined. Class 1, type A and B bituminous

Table 1. Results of regression analysis for SN versus day of year, by pavement section.

Section	SN_a	ΔSN	D_l	D_h	R^2	E_s
1	43.5	8.0	248	65	0.735	3.6
2	52.7	5.8	252	69	0.587	3.6
3	37.0	7.0	248	66	0.391	6.7
4	36.8	6.6	253	70	0.492	5.1
5	53.7	2.4	226	44	0.234	3.6
6	65.0	1.6	222	39	0.156	2.9
7	41.8	5.1	225	43	0.588	2.9
8	51.6	3.5	248	65	0.463	2.7
9	49.0	8.1	246	63	0.670	4.2
10	60.2	4.0	260	78	0.335	4.0
11	49.6	2.7	238	55	0.191	4.2
12	48.9	3.0	256	73	0.177	5.0
13	36.6	3.9	231	49	0.282	4.5
14	43.4	4.7	206	24	0.318	5.1
15	42.1	2.2	315	132	0.223	3.0
16	46.3	2.3	190	7	0.175	3.5
17	38.0	6.8	231	49	0.640	3.8
18	40.5	5.9	215	33	0.509	4.3
19	45.2	3.8	207	25	0.408	3.5
20	43.8	5.1	207	25	0.720	2.4

Note: D_h = day of year at which SN is highest ($D_h = D_l - 182.5$); R^2 = coefficient of correlation; E_s = standard error of the estimate.

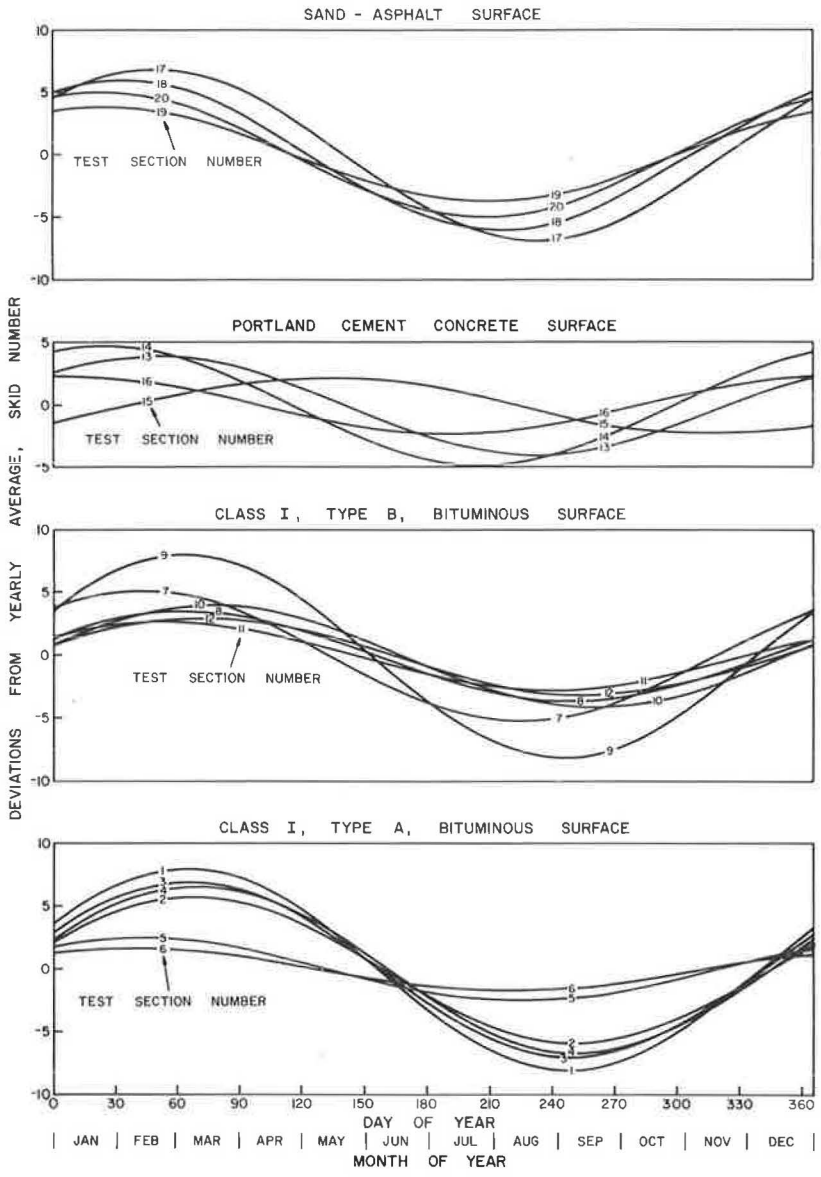

Figure 1. Best-fit curves for SN variation versus day of year for each test section, by pavement type.

Table 2. Results of regression analysis for deviations from yearly average SN versus day of year.

Pavement Type	SN_a	ΔSN	D_l	D_h	R^2	E_s
Class 1, type A	-0.1	5.3	248	65	0.402	4.8
AADT > 3500	0.0	6.8	250	68	0.508	5.0
AADT < 3500	0.0	2.0	225	42	0.198	3.2
Class 1, type B	0.1	4.1	243	61	0.346	4.1
AADT > 3500	-0.1	5.6	239	56	0.536	3.6
AADT < 3500	0.1	3.1	251	68	0.215	4.3
PCC	0.0	2.5	223	40	0.150	4.2
Sand-asphalt	0.0	5.4	218	36	0.537	3.7

pavements were also divided into two groups: AADT greater than or less than 3500 vehicles per day per lane. The equations and their coefficients are given in Table 2. Regression curves for the 365-day cycle are given in Figure 2. Data and curves are in Figures 3-5.

The regression curves indicated that SNs for class 1, type A that had the higher AADT varied seasonally by 14 points; the lowest SN occurred in early September. The SN for class 1, type A that had the lower AADT varied by 4 points, and the lowest SN value occurred in mid-August. The SN for class 1, type B surfaces that had the higher AADT varied seasonally by 11 points, and those with the lower AADT varied by 6. The lowest SN values for those pavements occurred in late August and early September, respectively. The SN for PCC pavements varied seasonally by 5 points. The lowest value occurred during mid-August. The SN for sand-asphalts varied seasonally by 11 points (lowest in early August).

PRECIPITATION AND TEMPERATURE VERSUS DAY OF YEAR

The mechanisms that change pavement surface characteristics are many and have been enumerated elsewhere (4). Two factors investigated in this study and that may be associated with these mechanisms were precipitation and temperature.

Since changes in the SN correlated with day of the year, factors associated with the principal mechanisms that cause variances must also correlate with day of the year. Figure 6 is a plot of monthly averages of precipitation and temperature. The amount and duration of precipitation and air

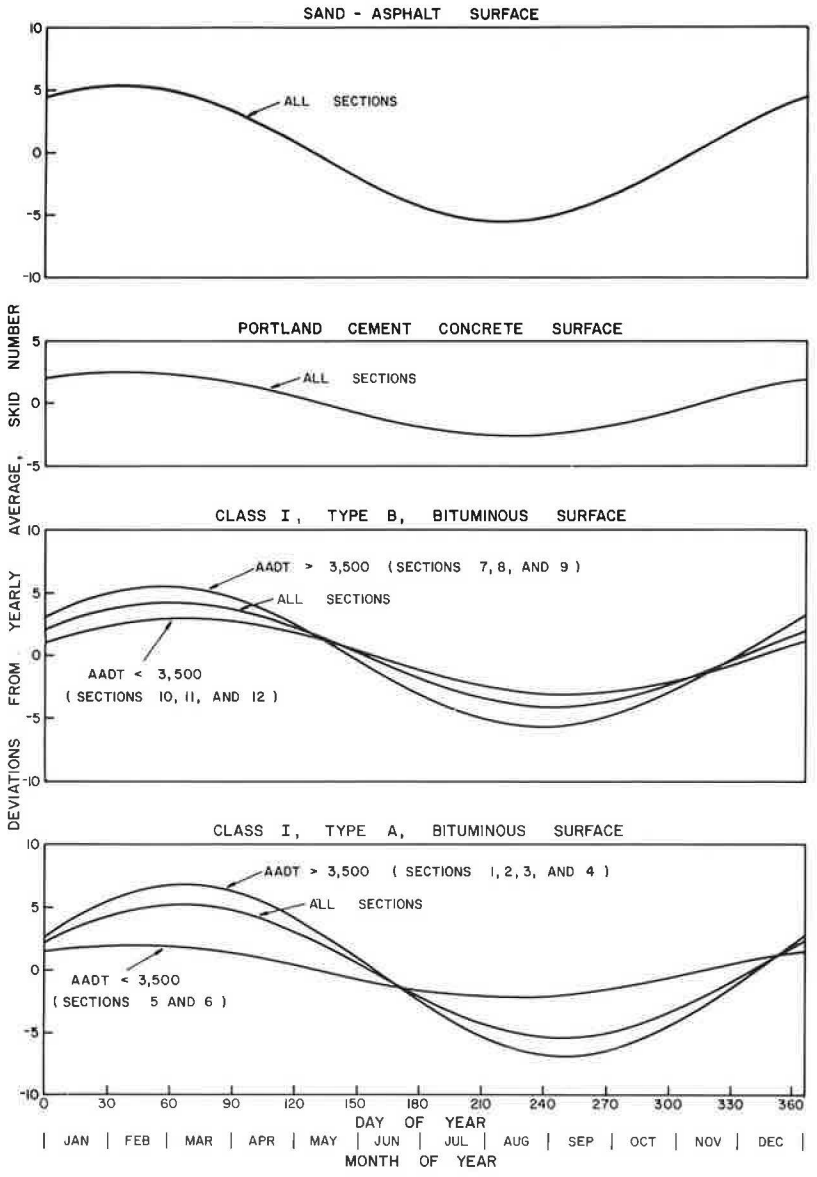

Figure 2. Best-fit curves for SN variation versus day of year for test sections grouped by pavement type.

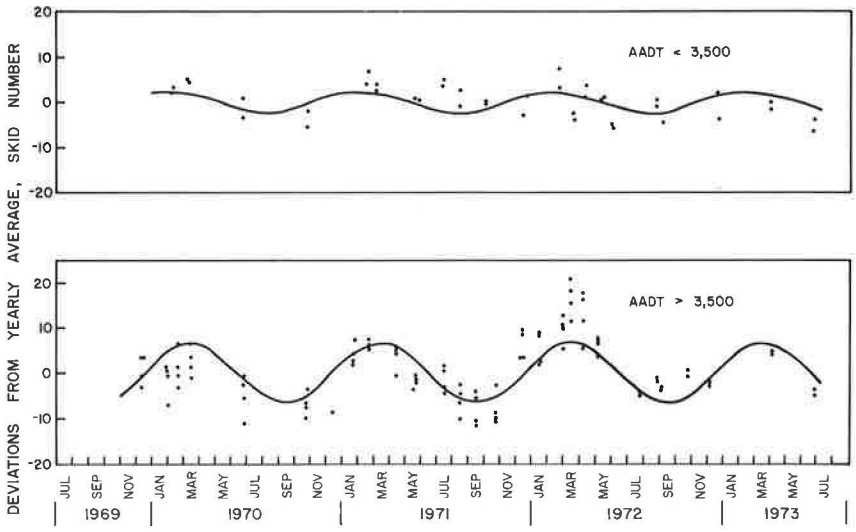

Figure 3. SN variation versus date of test for class 1, type A bituminous pavement, grouped by AADT.

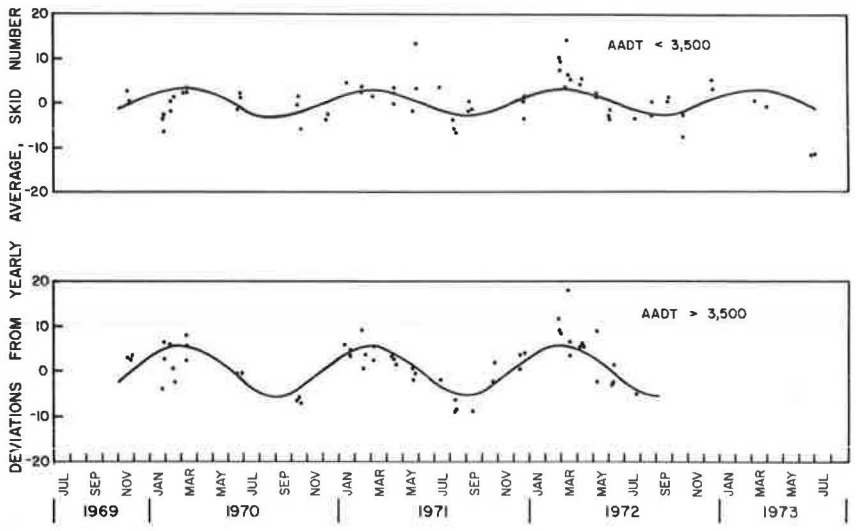

Figure 4. SN variation versus date of test for class 1, type B bituminous pavement, grouped by AADT.

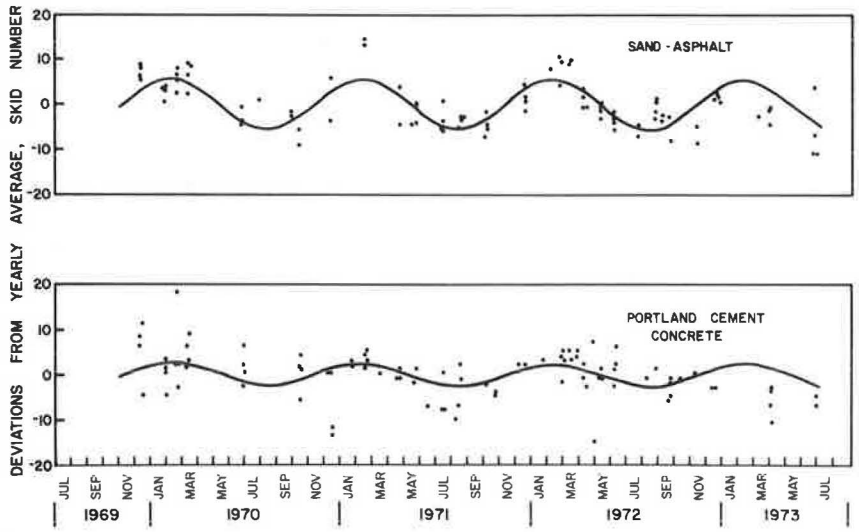

Figure 5. SN variation versus date of test for PCC and sand-asphalt pavements.

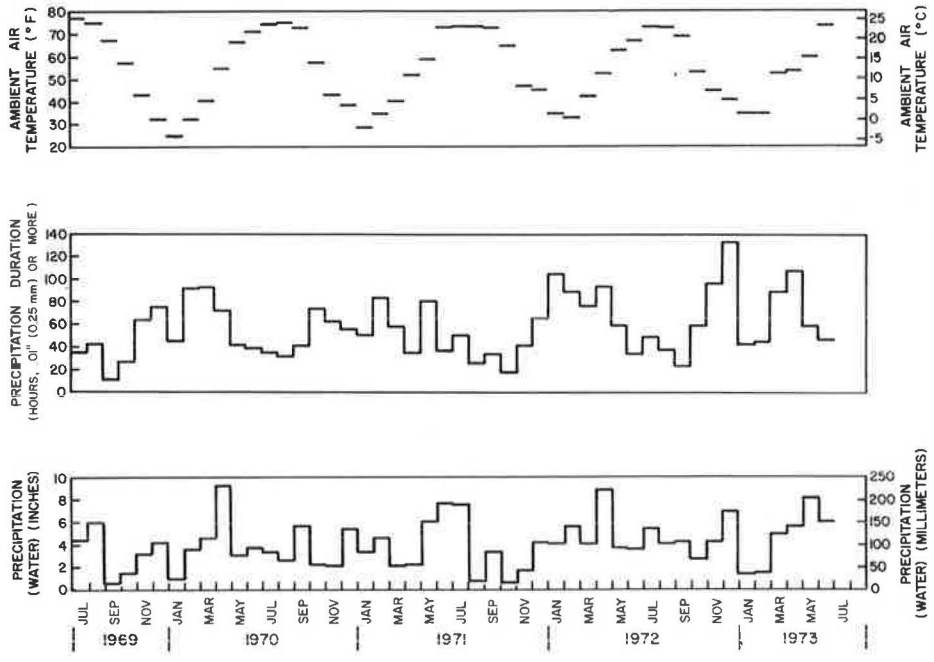

Figure 6. Average precipitation and temperature for each month of study period.

temperature correlated somewhat with month of the year.

Precipitation

Precipitation, given in Figure 6, was greatest during late spring and early summer and least during late summer and early fall. This trend was most evident in weekly averages throughout the four-year period, as shown in Figure 7. However, the amounts were highly variable; for example, both the largest and the smallest weekly averages occurred in early fall. The average duration of precipitation [number of hours per month that had 0.25 mm (0.01 in) or more], as shown in Figure 6, exhibited trends similar to the amounts of precipitation. The trend is illustrated more clearly in the weekly averages in Figure 8. The durations of precipitation were longest during mid-winter and were uniformly shortest from late spring to early fall. Average weekly durations (trace or more) were also determined for the four-year period. These are plotted in Figure 9 along with the best-fit cosine function. The best-fit curve indicated a good correlation between duration and day of the year. The trend was similar to that of variances in the SN versus day of the year. The longest and shortest periods of rainfall occurred from one-half to one month before the occurrence of the highest and lowest skid resistances, respectively. However, precipitation was not specific enough (not measured often enough) to permit correlations with changes in the SN.

Temperature

Monthly averages of air temperature during the period of study varied sinusoidally with month of the year (see Figure 6). Lowest temperatures occurred during January or February, and highest temperatures occurred during July or August. Temperatures for each test date were evaluated for relationships between temperature and day of the year.

Air temperature and pavement surface temperature were recorded at the time of skid testing. Regression analyses were performed by using these data for each type of pavement. The model equation was

$$T_p = T_a + \Delta T \cos [360^\circ(D - D_h)/365] \quad (2)$$

where

T_p = predicted temperature,
T_a = temperature about which T varies,
ΔT = variation of T about T_a,
D = day of year, and
D_h = day of year at which T is highest.

The results of the regression analyses are presented in Table 3. Good correlations were obtained in all cases. The lowest air temperature, 8°C (46°F), occurred in late January, and the highest, 28°C (82°F), was observed during the end of July. The lowest pavement surface temperature, 12°C (53°F), occurred during mid-January, and the highest, 38°C (101°F), was during mid-July. When these values were compared with the values in Table 2, the

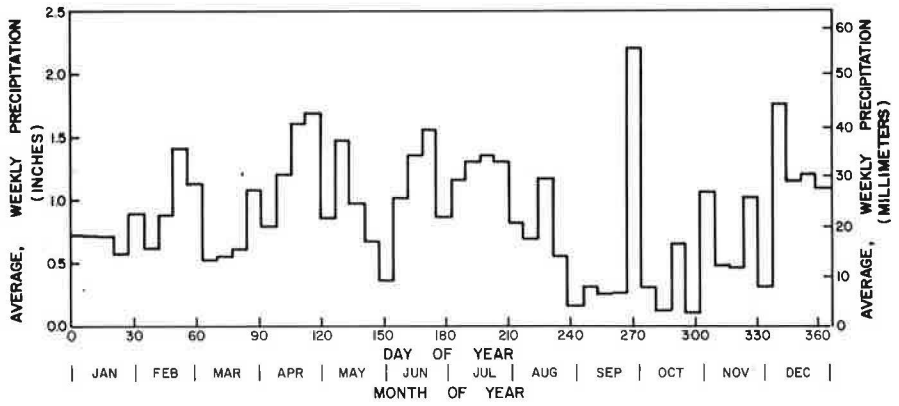

Figure 7. Average weekly precipitation for the combined four-year period.

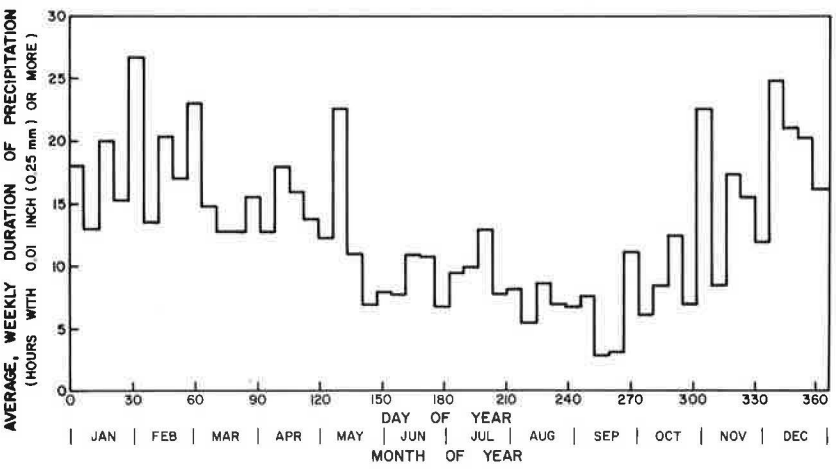

Figure 8. Average weekly duration of precipitation [0.25 mm (0.01 in) or more] for the combined four-year period.

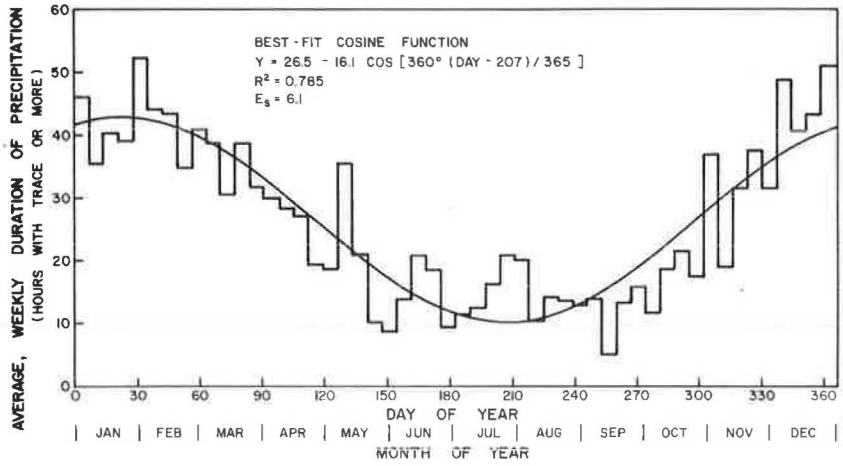

Figure 9. Average weekly duration of precipitation (trace or more) for the combined four-year period.

Table 3. Results of regression analysis for ambient air temperature and pavement surface temperature at time of skid testing versus day of year.

	Ambient Air Temperature						Pavement Surface Temperature					
Pavement Type	T_a (°C)	ΔT (°C)	D_h	D_l	R^2	E_s	T_a (°C)	ΔT (°C)	D_h	D_l	R^2	E_s
Class 1, type A	18.5	9.5	209	26	0.630	9.7	26.5	13.9	204	22	0.681	12.5
AADT > 3500	19.0	9.2	206	24	0.610	9.7	26.5	13.7	207	25	0.669	12.5
AADT < 3500	17.4	10.4	211	29	0.706	9.4	26.4	14.7	198	16	0.708	12.6
Class 1, type B	17.0	9.7	211	28	0.593	10.4	24.2	11.8	197	14	0.575	12.8
AADT > 3500	17.8	11.0	209	26	0.670	9.7	25.2	13.8	200	17	0.661	12.4
AADT < 3500	16.8	8.1	213	30	0.537	9.9	23.6	10.3	195	13	0.510	12.9
PCC	18.1	11.2	210	28	0.698	9.3	23.5	14.8	194	11	0.746	10.7
Sand-asphalt	17.6	10.1	212	29	0.636	10.1	24.7	12.6	194	12	0.592	13.6
All	17.8	9.9	210	28	0.633	9.8	24.9	13.2	198	16	0.638	12.7

Note: $t°C = (t°F - 32)/1.8$.

Table 4. Results of regression analysis for ambient air temperature averaged over various periods prior to skid testing versus day of test.

Weeks Prior to Skid Testing	T_a (°C)	ΔT (°C)	D_h	D_l	R^2	E_s
1	12.8	12.3	212	30	0.917	4.8
2	12.5	12.0	212	30	0.944	3.8
3	12.2	12.3	215	33	0.935	4.2
4	12.1	12.4	219	37	0.958	3.7
8	12.2	12.1	233	51	0.968	2.8

Note: $t°C = (t°F - 32)/1.8$.

highest and lowest SN values lagged the periods of lowest and highest temperature by one-half to one and one-half months. If the principal mechanism in changing skid resistance was associated with air or pavement temperature, then the reaction of that mechanism to temperature changes must have occurred over a period of a few weeks.

Air temperatures were averaged over periods of one, two, three, four, and eight weeks prior to the date of test. Correlations of these averages with day of test (based on a one-year cycle) were made by regression analysis. Results are presented in Table 4. The results indicated excellent correlations between air temperature, as averaged, and day of the year. A comparison of Table 4 with Table 2 indicated that days of highest and lowest SN agreed more closely with the days of highest and lowest temperature for the four-week and eight-week periods: the four-week period matched the fine-textured PCC, sand-asphalt, and the low-volume, class 1, type A surface; the eight-week period matched more closely the other types of pavements.

SN VERSUS TEMPERATURE

The similarity between temperature cycles and skid-resistance cycles indicated that temperature may be the primary factor that seasonally alters pavement surface characteristics and therefore alters skid resistance of the surface. In that case, the SN obtained should correlate with air or pavement surface temperature. A regression analysis of the SN versus several measures of temperature was made for each test section. The linear model equation used was

$$SN_p = SN_i + \Delta SN_t T \quad (3)$$

where

SN_i = SN at 0°C (or 0°F),
ΔSN_t = change of SN_i per 1°C (or 1°F), and
T = temperature.

As expected, the best correlations were found for pavements that also showed the best correlations between SN and day of the year (see Table 1). Also, in general, the best correlations were obtained with air temperature, averaged for either a four- or eight-week period prior to the day of testing. Additional analyses were made to determine whether grouping the test sections by pavement type improved the correlation between the SN and temperature. The measure of temperature used in this analysis was air temperature averaged over four- and eight-week periods prior to the day of testing. The SN_p's were calculated for test sections by using 21°C (70°F) for each measure of temperature. The corresponding SN_p was subtracted from the measured SN. Test sections were grouped as before.

Table 5. Results of regression analysis for adjusted SN versus ambient air temperature.

Pavement Type	Four Weeks Prior to Testing						Eight Weeks Prior to Testing					
	SN_i at		ΔSN_i per				SN_i at		ΔSN_i per			
	0°F	0°C	1°F	1°C	R^2	E_s	0°F	0°C	1°F	1°C	R^2	E_s
Class 1, type A	14.8	8.1	−0.21	−0.38	0.307	5.3	16.4	9.4	−0.23	−0.41	0.337	5.2
AADT > 3500	17.9	9.6	−0.26	−0.47	0.358	5.7	20.3	11.5	−0.29	−0.52	0.424	5.4
AADT < 3500	7.0	3.8	−0.10	−0.18	0.250	3.1	7.4	4.7	−0.10	−0.18	0.234	3.1
Class 1, type B	11.4	6.3	−0.16	−0.29	0.268	4.5	12.1	7.1	−0.17	−0.31	0.274	4.5
AADT > 3500	14.7	8.0	−0.21	−0.38	0.417	4.1	15.4	8.8	−0.22	−0.40	0.403	4.2
AADT < 3500	7.9	4.4	−0.11	−0.20	0.154	4.5	8.6	5.2	−0.12	−0.22	0.171	4.4
PCC	7.9	4.4	−0.11	−0.20	0.151	4.4	8.0	4.6	−0.12	−0.22	0.143	4.6
Sand-asphalt	17.8	9.8	−0.25	−0.45	0.588	3.6	18.0	10.1	−0.26	−0.47	0.532	3.8
All	12.8	7.0	−0.18	−0.32	0.296	4.7	13.6	8.0	−0.19	−0.34	0.294	4.8

Figure 10. Percent deviation from AADT versus day of year.

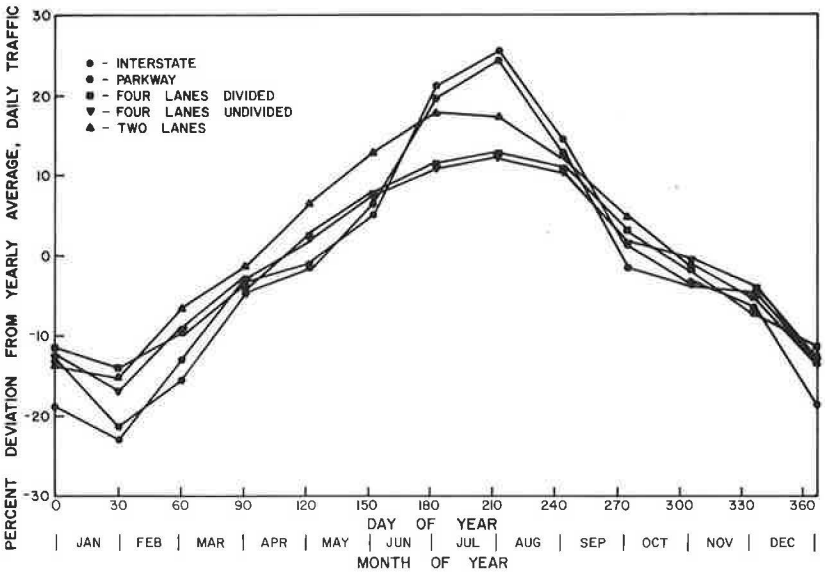

Regression analyses of this adjusted SN versus each average of air temperature were made. The results are presented in Table 5.

Results indicated that correlations between skid resistance and temperature were not so good as correlations between skid resistance and day of the year. For these data, therefore, prediction of the skid-resistance cycle based on correlations between SN and temperature would not be so accurate as those that used day of the year. This may mean that other factors have confounded the relationship between changes in skid resistance and temperature.

Inasmuch as changes in the SN were associated with traffic volume, deviations from AADT may be a significant factor. Monthly volume was determined from data presented by Agent, Herd, and Rizenbergs (5). These averages were converted to percent deviations from AADT and plotted versus day of year in Figure 10. These deviations were included as a second variable in the regression analyses of the SN and temperature. The linear model equation was

$$SN_p = SN_i + \Delta SN_t T + \Delta SN_a A \quad (4)$$

where

SN_i = SN at mean AADT and at 0°C (or 0°F),
ΔSN_a = change in SN_i per 1 percent deviation from AADT, and
A = percent deviation from AADT.

Results indicated that correlations between skid resistance and the combined variables of temperature and fluctuations of traffic volume were as good as correlations between skid resistance and day of the year. Equations for the best correlation for each pavement section are presented in Table 6. The SN was predicted by using these equations and temperature and traffic-volume values determined for selected days of the year. Temperature values were determined from the equations in Table 5. Traffic deviations were determined from the curves in Figure 8. SN_p fits the data at least as well as the equations that relate skid resistance to day of the year.

SUMMARY AND CONCLUSIONS

The seasonal variations of four types of pavements in Kentucky exhibited an annual sinusoidal cycle. When test sections at the same location (shoulder and lane versus median lane) were compared, the magnitude of the annual variation in skid resistance was strongly associated with volume of traffic. Lanes that had the greater traffic experienced the largest annual variation in skid resistance. Adjacent lanes that had like volumes experienced about the same annual variation. When sections at different locations were compared, those with the higher AADT did not necessarily exhibit the greatest changes in SN. Other factors apparently confounded the correlation.

The lowest SN during the year for PCC and sand-asphalt pavements occurred in early to mid-August. The lower SN for class 1 surfaces occurred in late August to early September. The change in

Table 6. Best correlation for each pavement section.

Section	Weeks Prior to Testing	SN at Mean AADT and at 0°F	SN at Mean AADT and at 0°C	SN per 1°F	SN per 1°C	SN per 1% AADT	R^2	E_s
1	1	85.7	61.1	−0.77	−1.39	+0.54	0.743	3.6
2	1	82.6	65.3	−0.54	−0.97	+0.39	0.554	3.8
3	8	55.6	44.4	−0.35	−0.63	+0.09	0.324	7.2
4	8	55.5	44.3	−0.35	−0.63	+0.13	0.413	5.6
5	3	70.2	60.6	−0.30	−0.54	+0.24	0.417	3.2
6	3	73.5	68.4	−0.16	−0.29	+0.09	0.230	2.9
7	4	53.3	46.6	−0.21	−0.38	+0.01	0.542	3.2
8	4	67.1	57.8	−0.29	−0.52	+0.31	0.499	2.7
9	8	73.2	58.8	−0.45	−0.81	+0.15	0.599	4.7
10	8	76.0	66.4	−0.30	−0.54	+0.19	0.350	4.1
11	2	63.0	55.0	−0.25	−0.45	+0.19	0.208	4.2
12	4	62.9	54.3	−0.27	−0.49	+0.27	0.181	5.1
13	8	42.8	39.3	−0.11	−0.20	−0.08	0.285	4.6
14	1	59.3	50.0	−0.29	−0.52	+0.09	0.379	5.0
15	3	60.0	49.4	−0.33	−0.59	+0.64	0.330	2.9
16	3	48.8	47.2	−0.05	−0.09	−0.08	0.165	3.6
17	4	65.8	49.5	−0.51	−0.92	+0.40	0.713	3.5
18	3	58.9	48.0	−0.34	−0.61	+0.13	0.572	4.1
19	2	58.8	50.8	−0.25	−0.45	+0.11	0.530	3.2
20	4	52.9	47.5	−0.17	−0.31	−0.10	0.751	2.3

skid resistance of sand-asphalt and class 1 surfaces with higher volumes of traffic was about 12 points. The change in skid resistance of PCC and bituminous concrete pavements that had lower volumes of traffic was about 5 points.

Similarity of the annual precipitation and temperature cycle to the annual variations in skid resistance of pavements suggested that both precipitation and temperature affected skid resistance. Precipitation data were not specific enough for the location of each test section nor was skid resistance measured frequently enough to allow for correlations with changes in skid resistance. Correlations between changes in SN and temperature were best for ambient air temperature averaged for four- and eight-week periods prior to the date of test. This suggested that the annual changes in skid resistance resulted from a reaction of the surface to temperature over a period of a few weeks. However, correlations between changes in SN and temperature were not so high as correlations between SN and day of the year.

On the other hand, combining traffic volume in the form of deviations from AADT with temperature yielded correlations with SN that were as good as correlations between the SN and day of year. More-specific traffic volumes would surely enable even better correlations.

The differences in seasonal variations among pavements included in this study were sufficiently large to preclude determination of factors, based on surface type and traffic volume alone, that could be routinely applied in the adjustment or correction of the SN, whether obtained within or outside a normal period of testing during the year. Other more-specific influences must be identified and quantified. In the interim, measurements in Kentucky should be confined between the first of July and the middle of November. Measurements obtained within that period will not differ, on the average, by more than four SNs. However, frequent testing of the reference sections is recommended to define more specifically each year the beginning and ending date of the testing season. The data from the reference sections may also serve to estimate adjustments whenever it is necessary to test at other times.

ACKNOWLEDGMENT

The work reported in this paper was performed by the Division of Research, Kentucky Department of Transportation, in cooperation with the Federal Highway Administration. Contents of the paper reflect our views and not necessarily the official views or policies of the Kentucky Department of Transportation or the Federal Highway Administration.

REFERENCES

1. R. L. Rizenbergs and H. A. Ward. Skid Testing with an Automobile. HRB, Highway Research Record 189, 1967, pp. 115-136.
2. J. L. Burchett and R. L. Rizenbergs. Pavement Slipperiness Studies. Division of Research, Kentucky Department of Highways, Frankfort, Rept. 292, March 1970.
3. R. L. Rizenbergs, J. L. Burchett, and C. T. Napier. Skid-Test Trailer: Description, Evaluation, and Adaptation. Division of Research, Kentucky Department of Highways, Frankfort, Rept. 338, Sept. 1972.
4. J. M. Rice. Seasonal Variations in Pavement Skid Resistance. Public Roads, Vol. 40, No. 4, March 1977, pp. 160-166.
5. K. R. Agent, D. R. Herd, and R. L. Rizenbergs. First-Year Effects of the Energy Crisis on Rural Highway Traffic in Kentucky. TRB, Transportation Research Record 567, 1976, pp. 70-81.

Experimental Investigation of the Transient Aspect of Hydroplaning

S. K. AGRAWAL AND J. J. HENRY

When a nonrotating tire moves from a quasi-dry section to a flooded section of a pavement, a transition from a nonhydroplaning to a hydroplaning state may occur. During this transition, friction force drops from a higher level to a lower level. This transition phenomenon was investigated experimentally. The experimental program was conducted both in the laboratory on a moving-belt friction tester and on the highways at the Pennsylvania Transportation Institute Research Facility. Good agreement was found between the laboratory and the highway test results. The results showed that the transition time could last up to 65 ms under the limits of operating conditions employed in the test program. The operating conditions included the test speed, the water-film thickness, the tire-inflation pressure, the vertical load on the tire, and the microtexture of the pavement.

When a film of water on a pavement is of sufficient thickness, the vehicle may hydroplane; i.e., the tires may be separated from the pavement by the water wedge formed between the tire surface and the pavement surface.

When a tire rolls or slides on a water-covered pavement at a velocity well below that at which hydroplaning occurs, most of the water is displaced from the contact region between tire and pavement by means of a forward and a lateral spray. The resulting change in momentum of the fluid creates hydrodynamic pressure that reacts on the surfaces of both pavement and tire. The force from hydrodynamic pressure increases as the square of the velocity, and also, as the velocity increases, the fluid inertia effects tend to retard fluid escape from the contact region between tire and pavement. The fluid wedge, which forms at the leading edge of the contact with the pavement, now becomes thicker and begins to penetrate farther into the contact region, so that part of the tire becomes supported by a progressively thicker water film. As the velocity increases further, the force from hydrodynamic pressure developed under the tire eventually exceeds the total vertical force and the tire will lift completely off the pavement. The lowest velocity at which this occurs is called the critical hydroplaning speed.

TRANSIENT ASPECT OF HYDROPLANING

The friction force developed by a tire will vary with time if the tire encounters water films of changing thickness along its path. Pavement unevenness causes the formation of random puddles on the pavement surface during precipitation. The unevenness may be the result of compaction by vehicular traffic on flexible pavements. Large temperature variations may cause the development of undulations in the pavement that create both longitudinal and transverse puddles.

The probability is large that skidding produced by moments about the yaw axis will occur because of differential braking or cornering forces developed when all the tires do not hydroplane. The question therefore arises whether hydroplaning occurs as soon as the tire encounters a deep puddle or only after a finite time interval has elapsed. This question leads to another: Is there a relationship between the puddle length and depth and the delayed response time (or transient duration)?

A large amount of work, both experimental (1,2) and analytical (3,4), has been done on the problem of hydroplaning, although exclusively for the case of a constant water layer on the pavement. The present research was necessary to determine whether there is a minimum puddle length that can exist on a pavement without creating a potential hazard to automotive traffic from temporary hydroplaning.

EXPERIMENTAL PROGRAM

The experimental program was designed to conduct tests by using full-scale passenger car tires both in the laboratory and on the highway. The operating variables were closely controlled in the laboratory, and the testing on the highways was done under prevailing highway and environmental conditions. In the entire test program the effects of the following variables were investigated:

1. Tire-inflation pressure,
2. Tire vertical load,
3. Sudden change in water-film thickness,
4. Magnitude of the sudden change in water-film thickness,
5. Surface texture,
6. Vehicle speed, and
7. Viscosity of water (by changing the temperature of water).

LABORATORY TEST PROGRAM

The laboratory test apparatus, henceforth called the moving-belt friction tester (MBFT), consists of an endless belt that runs on two steel drums. The roles of tire and pavement are reversed in the laboratory; i.e., the wheel that carries the test tire is held stationary in space, whereas the "pavement" moves relative to the fixed tire. The pavement is represented by a thin stainless-steel belt. The drums are supported on a rigid frame by means of four bearings. A flat Teflon plate under the belt supports the loaded tire. Figure 1 shows a schematic of the MBFT, and Figure 2 shows the tire-belt contact region. [Figures 1 and 2 are from Agrawal (5).] One drum is driven by an automotive engine, and belt tangential speeds of up to 110 km/h (70 miles/h) can be attained. The water-delivery system can provide a film thickness of up to 2.5 mm (0.1 in).

During each test the belt was sprayed with a thin film of water to represent quasi-dry conditions. A sudden change in the water-film thickness on the belt was brought about by engaging the water pump to the driving engine via a clutch. High-speed motion pictures of the flow through the nozzle showed that approximately 5-8 ms elapsed between the clutch engagement and the discharge through the nozzle. During this period, intermittent water jets were ejected from the nozzle. These water jets hit the tire surface and were deflected to the sides. It was noted that the friction force did not vary from the value at the quasi-dry condition, which indicated that the transient duration was not affected by these water jets.

The MBFT is instrumented to measure the following quantities:

Figure 1. Details of MBFT.

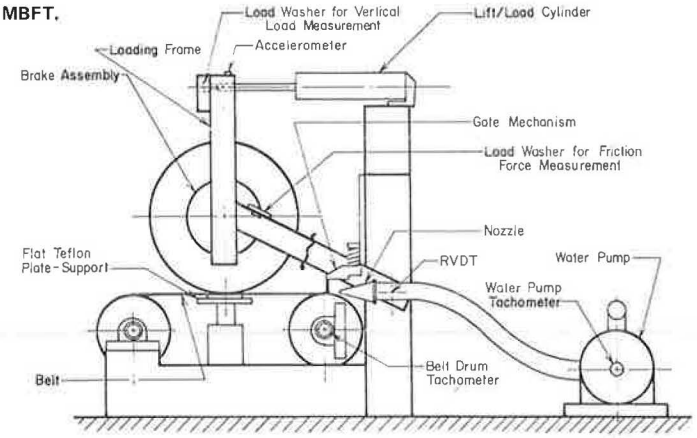

Figure 2. Belt support system and circumferential grooves on drums of MBFT.

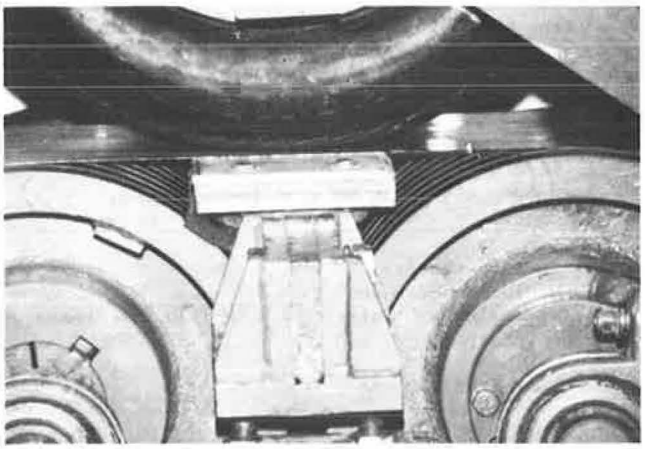

1. Vertical force on the tire,
2. Friction force at the tire-belt interface,
3. Rotational speed of the water pump, and
4. Vertical motion of the tire center.

In addition, a microswitch lever was placed ahead of the nozzle to indicate the precise instant of the impact of the thick film of water on the tire surface.

The following test conditions were selected:

1. Locked (completely braked) test tire,
2. Smooth bias-ply tire [approximately 0.66 m (26 in) in diameter] from which the tread was removed mechanically,
3. Tire-inflation pressure of 120-207 kPa (18-30 lbf/in^2),
4. Tire vertical force of 2000 N (450 lbf),
5. Belt speed of 48-110 km/h (30-70 miles/h),
6. Flow rate of water of 380-760 L/min (100-200 gal/min),
7. Water temperature of 10°C (50°F) and 35°C (95°F), and
8. Fine-textured belt (metallic spray coating).

The friction force at the tire-belt interface is represented as the brake-force coefficient (BFC), defined as follows:

$$BFC = [(\text{friction force})/(\text{vertical force})] \times 100 \quad (1)$$

Test Procedure

A complete test sequence required two operators and consisted of the following steps:

1. Apply the brake to keep the tire from rotating;
2. Preselect the vertical force and adjust the pneumatic pressure in the loading cylinder;
3. Adjust the tire-inflation pressure;
4. Obtain the preselected belt speed;
5. Apply the thin film of water on the moving belt to simulate quasi-dry condition;
6. Bring the tire down on the belt and apply the vertical force;
7. Start the recording equipment;
8. Engage the clutch to supply thick water film;
9. Lift the tire, stop the belt, and disengage the water pump; and
10. Stop the recording equipment.

Test Results and Discussion

The typical force-time history as the tire encountered a sudden change in the water-film thickness is shown in Figure 3. To describe the response of the tire to the change in film thickness, three time periods are defined, as follows: τ_1, the time to reach the first steady-state friction (BFC) value; τ_2, the time to reach minimum friction value; and τ_3, overall time of the transient.

Total hydroplaning in the laboratory tests was indicated by a small BFC value. The final available BFC for total hydroplaning is very small (typically less than 5 percent of the vertical force, or a friction coefficient of 0.05). Under a total hydroplaning condition, the tire is completely separated from the pavement. Whether one actually achieves total hydroplaning depends on the thickness of the water film, the speed, the texture of the surface, the condition of the tire, and other operating variables. In fact, since the operating conditions were varied in the tests, hydroplaning in the final state did not always occur. However, even when the final state is not one of total hydroplaning, the nature of the response is the same and can be described by the same three characteristic times. The operating conditions tested are described in Table 1.

Table 2 shows the effects of tire-inflation pressure, water-flow rate, and water temperature on the transient times. Under each set of operating conditions, the testing was conducted in an increasing order of belt speed. It can be seen that the increase in speed under a fixed set of other

Figure 3. Typical force-time history.

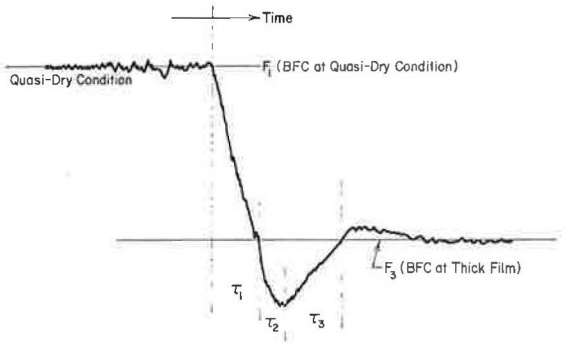

Table 1. Operating conditions for laboratory tests.

Test	Tire-Inflation Pressure (lbf/in^2)	Flow Rate (gal/min)	Water Temperature (°F)
2A-C	24	184	50
3A-E	18	128	50
4A-D	18	184	50
5A-D	35	128	50
6A-C	24	194	50
7A-E	18	136	50
8A-D	18	200	50
10A-C	18	185	95
11A-C	18	172	95
12A-D	24	200	95
13A-D	18	128	95

Notes: 1 lbf/in^2 = 6.8 kPa; 1 lbf = 4.4 N; 1 gal/min = 3.8 L/min; $t°F = (t°C \div 0.55) + 32$.
For all tests, tire vertical load was 440 lbf, and a belt that had a textured surface was used.

operating conditions does not show a significant variation in the three transient-time durations.

The gross effects of changing flow rates, viscosity, and inflation pressure are investigated in Table 3, which shows the average values of the transients for each set of test conditions. Test group A consists of tests 10 A-C, 11 A-C, and 13 A-D. No significant variation or trend is identifiable in the average transient durations of τ_1, τ_2, and τ_3. Group B represents similar results when the water temperature (hence viscosity) was changed. Again no significant variation or trend is identifiable. Group C represents the effect of viscosity change in which the effect of flow rates (groups A and B) is insignificant. Again the transient-time durations are very close. The last row in Table 3 represents the combined effect of all the operating variables. It can be seen that the magnitudes of τ_1, τ_2, and τ_3 are all of the same order when compared with the corresponding durations in each of the other test groups. Thus it can be concluded that the transient durations or the response times are not sensitive to changes in operating variables.

Referring again to Table 2, it should be noted that, in each test series, the steady-state value of the BFC in the flooded region (F_3) decreases with increasing speed. This trend is well documented for highway testing (6). However, whereas in the highway testing the film thickness on the pavement remains constant for a series of tests in which the speed is increased gradually from one test to another, the film thickness in the laboratory changes when belt speed is increased if the water-flow rate remains constant. If the changes in the film thickness during a test series are ignored, the laboratory tests show the trend documented earlier (6).

HIGHWAY TEST PROGRAM

The Pennsylvania Transportation Institute road friction tester (Mark 3) (7) was the principal test apparatus. It is equipped with a six-component force-and-torque measurement system.

The tester has a single wheel. The trailer consists of a frame, a passenger car brake-and-wheel assembly, a rod that retains the brake plate (otherwise free to rotate), and an air cylinder for providing normal force on the tire. The wheel spindle is mounted rigidly to the main frame, and the frame is connected by pitch-and-yaw pivots to the hitch of the towing vehicle.

To obtain a sudden change in the water-film thickness in the path of the tire, water was discharged on the pavement in the lateral direction to create a flooded or thick-film region and to mildly wet the pavement section outside the flooded region. Figures 4 and 5 show the tester and the preparation of the test site. Figures 6 and 7 show a distinct step change in the film thickness and the tester in operation.

The tester is instrumented to measure the following quantities: (a) longitudinal forces at the tire-pavement interface, (b) vertical force on the tire, and (c) vehicle speed.

The water-film thickness on the pavement was measured by using a National Aeronautics and Space Administration water-level-depth gauge. In addition, a microswitch was installed on the tester to indicate the precise instant that the test tire comes in contact with the line of sudden change in water thickness.

The following test conditions were selected:

1. Locked (i.e., completely braked) test tire,
2. ASTM standard E524 tire,
3. Tire-inflation pressure of 120-270 kPa (18-30 lbf/in^2),
4. Tire vertical force of 1780-4450 N (400-1000 lbf),
5. Vehicle speed of 40-96 km/h (25-60 miles/h),
6. Water-film thickness of 1.27-6.35 mm (0.05-0.25 in), and
7. Pavement texture of 0.38-0.76 mm (0.015-0.03 in).

When a desired film thickness was attained on the pavement, repeated tests were conducted by using increasing vehicle speeds. The highest speed of test was limited by either the available approach length or the minimum drag force attainable on a particular pavement surface. A series of tests was performed by using different combinations of operating conditions.

Test Results and Discussion

The typical force-time history in the highway tests (Table 4) was similar to that in the laboratory test program.

Table 5 shows the effect of the various test parameters on the transient-time durations (τ_1, τ_2, and τ_3) and on the friction force. C2, C3, and C5; D1-D10; and J1-J4, J6-J12, and J16-J19 in Table 4 refer to data obtained on portland cement concrete (PCC), Jennite, and bituminous concrete surfaces (ID2A), respectively. The surfaces differ in method of construction, material used, and available texture.

Total hydroplaning condition in the highway test program was identified by a small value of BFC, as was done in the laboratory tests. The reason for

Table 2. Laboratory-test results on a textured belt.

Belt Speed (miles/h)	Transient Time (ms) τ_1	τ_2	τ_3	BFC F_1	F_2	F_3	Distance (ft) d_1	d_2	d_3
Tests 2A-C									
43	2.0	5.9	42.0	18.2	–	6.8	0.13	0.37	2.65
46	3.9	7.8	–	18.2	–	5.7	0.26	0.53	–
49	3.0	6.8	33.2	17.0	–	4.6	0.21	0.48	2.39
Avg	3.0	6.8	37.6						
Tests 3A-E									
28	9.7	15.6	27.3	27.3	–	17.0	0.40	0.64	1.12
36	8.8	14.6	27.3	20.5	–	10.2	0.47	0.77	1.47
39	5.9	9.8	27.3	21.6	–	8.4	0.34	0.56	1.56
44	4.9	9.8	31.3	18.2	–	6.8	0.32	0.63	2.02
48	5.9	8.8	25.4	19.3	–	5.7	0.41	0.62	1.80
Avg	7.0	11.7	27.7						
Tests 4A-D									
34	3.9	–	–	18.2	–	9.1	0.20	–	–
40	–	–	–	13.6	–	6.8	–	–	–
45	5.9	11.7	31.3	21.6	–	4.6	0.39	0.78	2.06
50	5.9	7.8	21.5	18.2	–	2.3	0.43	0.57	1.58
Avg	5.2	9.8	26.5						
Tests 5A-D									
30	7.8	14.7	27.3	30.7	–	18.2	0.35	0.65	1.20
38	2.9	6.9	12.7	20.5	–	8.0	0.16	0.38	0.71
44	10.7	16.6	25.4	19.3	–	7.9	0.69	1.10	1.64
48	2.9	8.8	–	18.2	–	5.7	0.21	0.62	–
Avg	6.1	11.5	21.8						
Tests 6A-C									
30	9.8	17.6	47.9	38.6	–	19.3	0.43	0.77	2.11
42	11.7	18.6	39.1	15.9	–	6.8	0.72	1.14	2.40
52	4.9	9.8	15.6	27.3	–	2.3	0.37	0.75	1.19
Avg	8.8	15.3	34.2						
Tests 7A-E									
34	2.9	7.8	15.6	27.3	–	11.4	0.15	0.39	0.78
38	2.9	7.8	13.7	19.3	–	7.9	0.16	0.44	0.76
42	5.9	12.7	–	19.3	–	9.1	0.36	0.78	–
44	9.8	16.6	22.5	18.2	–	5.7	0.63	1.07	1.45
50	8.7	10.7	15.7	15.9	–	3.4	0.64	0.78	1.15
Avg	6.1	11.1	16.9						
Tests 8A-D									
30	9.8	14.7	31.3	30.7	–	10.2	0.43	0.65	1.38
38	8.8	13.7	17.6	19.3	–	5.7	0.49	0.76	0.98
42	4.9	8.7	17.6	15.9	–	4.6	0.30	0.60	1.08
50	9.8	13.7	20.5	20.5	–	2.27	0.72	1.00	1.50
Avg	8.3	12.7	21.8						
Tests 10A-C									
34	5.8	9.8	31.3	18.2	–	11.4	0.30	0.49	1.60
42	5.9	11.7	30.3	11.4	–	3.4	0.36	0.72	1.90
48	9.8	19.5	28.3	8.0	–	0	0.69	1.38	2.00
Avg	7.2	13.7	30.0						
Tests 11A-C									
32	–	–	–	19.3	–	9.1	–	–	–
49	4.9	9.8	16.6	12.5	–	4.5	0.35	0.70	1.20
51	9.8	16.6	22.5	6.8	–	2.3	0.73	1.20	1.70
Avg	7.4	13.2	19.6						
Tests 12A-D									
32	7.8	16.6	19.5	20.5	–	12.5	0.37	0.78	0.92
38	6.8	9.8	17.6	18.2	–	9.1	0.38	0.54	0.98
42	–	–	–	15.9	–	8.0	–	–	10
48	3.9	7.8	15.6	13.6	–	4.6	0.30	0.60	1.10
Avg	6.2	11.4	17.6						
Tests 13A-D									
29	3.9	8.8	23.4	25.0	–	17.0	0.17	0.37	1.00
36	5.9	12.7	21.5	15.9	–	10.2	0.31	0.67	1.13
45	7.8	15.6	22.5	12.5	–	5.7	0.52	1.03	1.48
52	7.8	16.6	22.5	11.4	–	3.4	0.60	1.27	1.71
Avg	6.4	13.4	22.5						

Notes: 1 mile/h = 1.6 km/h; 1 ft = 0.33 m.
Dash indicates that data cannot be interpreted.

Table 3. Summary of laboratory-test results.

Test Group	Operating Condition Changed	Categories Compared	Average Transient Times (ms) τ_1	τ_2	τ_3	Conclusion
A	Flow rate (lower viscosity, low inflation pressure)	10A-C	7.2	13.7	30.0	No significant variation or trend
		11A-C	7.4	13.2	19.6	
		13A-D	6.4	13.4	22.5	
		Avg	7.0	13.4	24.0	
B	Flow rate (higher viscosity, low inflation pressure)	4A-D	5.2	9.8	26.5	No significant variation or trend
		8A-D	8.3	12.7	21.8	
		7A-E	6.1	11.1	16.9	
		3A-E	7.0	11.7	27.7	
		Avg	6.7	11.3	23.2	
C	Flow rate (higher viscosity, higher inflation)	2A-C	3.0	6.8	37.6	Small variation in τ_1 and τ_2
		6A-C	8.8	15.3	34.2	
		Avg	5.9	11.1	35.9	
D	Viscosity (similar flow rates, higher inflation pressure)	12A-D	6.2	11.4	17.6	No significant variation
		6A-C	8.8	15.3	34.2	
		Avg	7.5	13.4	25.9	
E	Viscosity	A	7.0	13.4	24.0	
		B	6.7	11.3	23.2	
		Avg	6.9	12.4	23.6	
	Inflation pressure	C	5.9	11.1	35.9	
		E	6.9	12.4	23.6	
	Combined effect	All	7.4	11.2	29.6	

Note: 1 gal/min = 3.8 L/min; 1 lbf/in^2 = 6.8 kPa.

using this criterion was the fact that the transient-time durations did not show a significant variation with speed under any set of operating conditions (Table 3).

Figure 4. Mark 3 friction tester.

Figure 5. Preparation of test site.

To compare the effects of various parameters, the results from Table 5 are summarized in Table 6. Since the effect of vehicle speed can be ignored for each set of operating conditions (water-film thickness, tire-inflation pressure, vertical force, and texture depth), average values of the three transient-time durations are computed. The effect of water-film thickness, tire-inflation pressure, and

Figure 6. Distinct step change in film thickness.

Figure 7. Mark 3 friction tester during a test.

Table 4. Operating conditions for highway tests.

Test	Water-Film Thickness (in)	Tire-Inflation Pressure (lbf/in²)	Tire Vertical Load (lbf)	Pavement Characteristics		
				Surface Description	Texture Depth (in)	Skid No.
C2	0.075	30	800	PCC	0.018	36
C3		18	800	PCC	0.018	36
C5		24	800	PCC	0.018	36
D1	0.06	18	800	ID2A	0.030	57
D2		24	800	ID2A	0.030	57
D3	0.15	24	800	ID2A	0.030	57
D4		18	800	ID2A	0.030	57
D5	0.25	18	800	ID2A	0.030	57
D6		24	800	ID2A	0.030	57
D7		14	800	ID2A	0.030	57
D8	0.85	18	800	ID2A	0.030	57
D9		24	800	ID2A	0.030	57
D10		30	800	ID2A	0.030	57
J1	0.055	24	800	Jennite	0.015	16
J2		30	800	Jennite	0.015	16
J3		18	800	Jennite	0.015	16
J4		18	400	Jennite	0.015	16
J6		24	400	Jennite	0.015	16
J7	0.075	24	800	Jennite	0.015	16
J8		30	800	Jennite	0.015	16
J9		18	800	Jennite	0.015	16
J10		18	1000	Jennite	0.015	16
J11	0.10	30	800	Jennite	0.015	16
J12		24	800	Jennite	0.015	16
J16		24	1000	Jennite	0.015	16
J17	0.25	24	800	Jennite	0.015	16
J18		18	800	Jennite	0.015	16
J19		30	800	Jennite	0.015	16

Note: PCC = portland cement concrete; ID2A = bituminous concrete.

Table 5. Highway-test results on various surfaces.

Vehicle Speed (miles/h)	Transient Time (ms) τ_1	τ_2	τ_3	BFC F_1	F_3	Distance (ft) d_1	d_2	d_3
Test C2								
30	7.8	19.5	82.0	53.8	33.8	0.34	0.86	3.61
40	9.8	17.6	39.0	42.5	25.0	0.57	1.03	2.29
50	8.8	18.6	66.4	42.5	17.5	0.64	1.36	4.87
Avg	8.8	18.6	62.5					
Test C3								
31	13.7	23.4	82.0	56.3	36.3	0.62	1.06	3.73
39	11.7	21.5	46.9	57.5	25.0	0.67	1.23	2.68
50	7.8	15.6	25.4	50.0	20.0	0.57	1.14	1.88
Avg	11.1	20.2	51.4					
Test C5								
30	11.7	22.5	70.3	44.0	32.0	0.51	0.99	3.09
50	13.7	18.6	30.3	44.0	16.0	1.00	1.36	2.22
Avg	12.7	20.6	50.3					
Test D1								
34	11.7	17.6	25.4	50.0	22.5	0.58	0.88	1.27
44	15.6	23.4	27.3	42.5	15.0	1.01	1.51	1.76
51	13.7	19.5	25.4	40.0	7.5	1.02	1.46	1.90
Avg	13.7	20.2	26.0					
Test D2								
29	10.7	18.6	21.6	47.5	30.0	0.46	0.79	0.92
35	12.7	18.6	21.5	41.3	18.8	0.65	0.95	1.10
40	13.7	19.5	27.0	35.0	11.3	0.80	1.14	1.58
45	18.6	21.5	26.4	35.0	7.5	1.23	1.42	1.74
50	9.8	15.6	21.5	38.8	6.3	0.72	1.14	1.58
58	11.7	17.6	23.4	35.0	2.5	1.00	1.50	1.99
Avg	12.9	18.6	23.6					
Test D3								
32	7.8	14.6	21.5	42.5	20.0	0.37	0.69	1.01
32	11.7	19.5	23.4	47.5	20.0	0.55	0.92	1.10
35	11.7	18.6	23.4	43.1	15.0	0.60	0.95	1.20
35	11.7	17.6	23.4	42.5	17.5	0.60	0.90	1.20
42	9.8	15.6	20.5	42.5	7.5	0.60	0.96	1.26
Avg	10.5	17.2	22.6					
Test D4								
32	15.6	23.4	30.0	52.5	17.5	0.73	1.10	1.41
35	20.5	20.5	20.5	55.0	11.3	1.05	1.05	1.05
40	15.8	19.5	27.3	57.5	7.5	0.93	1.14	1.60
45	11.7	15.8	21.5	47.5	7.5	0.77	1.04	1.42
52	9.8	17.6	23.4	37.5	6.3	0.75	1.34	1.78
59	5.9	13.7	19.5	31.3	1.3	1.51	1.19	1.69
Avg	13.2	18.4	23.7					
Test D5								
32	13.7	19.5	23.4	40.0	15.0	0.64	0.92	1.10
36	18.5	18.5	18.5	38.8	7.5	0.98	0.98	0.98
41	23.4	23.4	23.4	35.0	7.5	1.41	1.41	1.41
46	9.8	15.7	23.4	35.0	5.0	0.66	1.06	1.58
51	9.5	19.5	25.4	35.0	3.8	0.71	1.48	1.90
58	7.8	17.6	23.1	32.5	2.5	0.67	1.50	1.97
Avg	13.8	19.0	22.9					
Test D6								
32	13.7	17.6	21.5	45.0	17.5	0.64	0.83	1.01
35	15.9	20.1	25.6	41.3	7.5	0.82	1.03	1.31
40	7.8	15.6	19.5	37.5	8.8	0.46	0.92	1.14
46	7.8	13.7	21.5	32.5	6.3	0.53	0.92	1.45
51	11.9	18.6	27.3	32.5	5.0	0.89	1.39	2.04
Avg	11.4	17.1	23.0					
Test D7								
36	9.8	17.6	21.5	32.5	15.0	0.52	0.93	1.14
Test D8								
35	12.7	16.6	29.3	50.0	18.8	0.65	0.85	1.50
40	24.4	29.3	32.1	45.0	12.5	1.43	1.72	1.88
45	11.7	18.6	23.4	42.5	10.0	0.77	1.23	1.54
51	7.8	15.3	21.5	52.5	10.0	0.58	1.14	1.61
57	9.8	18.6	25.4	40.0	5.0	0.82	1.55	2.12
Avg	13.3	19.7	26.3					
Test D9								
35	8.8	15.6	21.5	70.0	25.0	0.45	0.80	1.10
35	5.9	15.0	21.5	70.0	25.0	0.30	0.77	1.10
36	7.8	13.7	19.5	58.0	20.0	0.41	0.72	1.03
Avg	7.5	14.8	20.8					
Test D10								
38	10.7	15.6	19.5	51.3	20.0	0.60	0.87	1.09
40	9.8	13.7	21.5	44.4	16.3	0.57	0.80	1.26
45	22.5	27.3	31.3	46.3	11.3	1.49	1.80	2.07
50	13.7	18.6	22.5	35.0	8.8	1.00	1.36	1.65
55	10.7	19.5	25.4	37.5	5.0	0.86	1.57	2.05
Avg	13.5	18.9	24.0					
Test J1								
29	21.5	27.3	32.2	37.5	20.0	0.91	1.37	1.16
33	17.6	25.4	33.2	33.8	12.5	0.85	1.61	1.23
39	25.4	28.3	31.3	30.0	10.0	1.45	1.80	1.62
39	13.7	19.5	25.4	22.5	10.0	0.78	1.45	1.29
44	20.5	23.4	33.2	22.5	7.5	1.32	2.14	1.45
Avg	19.75	24.8	31.06					
Test J2								
29	19.5	19.5	32.2	38.1	15.6	0.83	1.37	0.83
29	17.6	27.3	36.1	35.0	16.3	0.75	1.53	1.16
34	13.7	20.5	29.3	35.0	13.8	0.68	1.46	1.02
39	13.7	17.6	25.4	28.8	8.8	0.78	1.45	1.01
45	13.7	19.5	37.1	30.0	7.5	0.90	2.45	1.29
Avg	15.6	20.9	32.0					
Test J3								
28	13.7	15.6	35.2	32.5	20.0	0.56	1.45	0.64
14	15.6	24.4	39.1	21.3	12.5	0.78	1.95	1.22
45	11.7	19.5	30.3	27.5	8.9	0.77	2.00	1.29
49	9.7	13.7	33.2	25.0	10.0	0.70	2.39	0.98
Avg	12.7	34.5	18.3					
Test J4								
30	11.7	15.6	21.5	35.0	20.0	0.95	0.51	0.69
40	15.6	23.4	35.1	25.0	7.5	0.91	1.37	2.06
45	15.6	23.4	39.0	39.0	7.5	1.03	1.54	2.57
Avg	14.3	20.8	31.9					
Test J6								
29	19.5	25.4	33.2	45.0	10.0	0.83	1.08	1.41
40	11.7	21.5	27.3	27.5	5.0	0.69	1.26	1.60
49	10.7	18.6	25.4	30.0	0.0	0.77	1.34	1.82
Avg	14.0	21.8	28.6					
Test J7								
29	15.6	25.4	33.2	30.0	7.5	0.66	1.08	1.41
39	15.6	19.5	29.3	17.5	3.8	0.89	1.11	1.68
45	11.7	15.6	25.4	27.5	2.5	0.77	1.03	1.68
40	9.8	17.6	27.3	27.3	2.5	0.72	1.29	2.00
34	15.6	20.5	31.3	23.8	6.3	0.78	1.02	1.56
Avg	13.7	19.7	29.3					
Test J8								
27	14.6	22.5	34.2	27.5	16.3	0.58	0.89	1.35
39	13.7	19.5	33.2	30.0	10.0	0.78	1.11	1.9
Avg	14.2	21.0	33.7					

Table 5 continued.

Vehicle Speed (miles/h)	Transient Time (ms) τ_1	τ_2	τ_3	BFC F_1	F_3	Distance (ft) d_1	d_2	d_3
Test J9								
32	11.7	18.6	34.2	42.5	13.8	0.55	0.87	1.60
40	13.7	24.4	29.3	35.0	8.9	0.80	1.43	1.71
44	7.8	15.6	26.4	36.9	8.9	0.50	1.00	1.70
49	5.8	13.8	25.4	35.0	7.5	0.42	0.99	1.82
Avg	9.8	18.1	28.8					
Test J10								
29	7.8	10.7	23.4	42.5	20.6	0.33	0.45	0.98
39	9.8	23.4	31.3	40.0	15.0	0.56	1.34	1.79
Avg	8.8	17.0	27.4					
Test J11								
29	7.8	19.5	31.3	27.5	12.5	0.33	0.83	1.33
39	13.7	–	31.5	23.8	7.5	0.78	–	1.80
44	8.8	19.5	31.1	17.5	3.8	1.57	1.26	2.01
49	11.7	–	31.3	17.5	1.3	0.84	–	2.25
Avg	10.5	19.5	31.3					
Test J12								
28	13.7	19.5	31.3	35.0	13.8	0.56	0.80	1.29
39	7.8	19.5	39.1	22.5	7.5	0.45	1.12	2.24
44	11.7	21.5	31.3	22.5	5.0	0.76	1.39	2.02
Avg	11.1	20.2	33.9					
Test J16								
39	7.8	19.5	27.3	16.0	8.0	0.45	1.12	1.56
44	11.5	23.4	35.2	–	5.0	0.74	1.51	2.27
49	17.6	29.3	35.1	14.0	4.0	1.26	2.11	2.53
54	17.6	26.4	33.2	18.0	2.0	1.39	2.09	2.63
Avg	13.6	24.7	32.6					
Test J17								
30	12.7	19.8	27.3	25.0	12.5	0.56	0.87	1.20
40	13.7	21.5	27.3	22.5	10.0	0.80	1.26	1.60
45	7.8	15.6	29.3	22.5	10.6	0.51	1.03	1.93
Avg	11.1	19.0	28.0					
Test J18								
33	19.5	25.4	31.2	31.3	12.3	0.94	1.23	1.51
36	11.7	18.6	27.3	30.0	10.0	0.62	0.98	1.44
41	14.6	18.6	23.5	30.0	8.3	0.88	1.12	1.41
46	11.9	17.6	26.4	22.5	5.8	0.80	1.19	1.78
52	10.7	18.6	27.3	–	7.5	0.82	1.42	2.08
Avg	13.5	19.8	27.1					
Test J19								
30	13.7	17.6	27.3	25.0	3.8	0.60	0.77	1.20
35	8.8	13.7	23.4	21.3	8.8	0.45	0.70	1.20
41	7.8	17.6	25.4	25.0	10.0	0.47	1.06	1.53
46	11.7	13.8	23.4	21.3	6.3	0.79	0.93	1.58
51	7.8	14.6	22.5	20.0	5.0	0.58	1.09	1.68
Avg	13.7	17.5	24.4					

Note: 1 mile/h = 1.6 km/h; 1 ft = 0.33 m.

Table 6. Summary of highway-test results.

Categories Compared	Transient Time (ms) τ_1	τ_2	τ_3	Categories Compared	Transient Time (ms) τ_1	τ_2	τ_3
C2	8.8	18.6	62.5	J6	14.0	21.9	28.6
C3	11.1	20.4	51.4	J7	13.7	19.7	29.3
C5	12.7	20.6	50.3	J8	14.2	21.0	33.7
Avg	10.9	19.9	54.7	J9	9.8	18.1	28.8
D1	13.7	20.2	26.0	J10	8.8	17.0	27.4
D2	12.9	18.6	23.6	J11	10.5	19.5	31.3
D3	10.5	17.2	22.6	J12	11.1	20.2	33.9
D4	13.2	18.4	23.7	J16	13.6	24.7	32.6
D5	13.8	19.0	22.9	J17	11.1	19.0	28.0
D6	11.4	17.1	23.0	J18	13.5	19.8	27.1
D8	13.3	19.7	26.3	J19	10.0	17.5	24.4
D10	13.5	18.9	24.0	Avg	12.8	18.7	30.2
Avg	12.8	18.6	24.0	D	12.8	18.6	24.0
J1	19.8	24.8	31.1	C	10.9	19.9	54.7
J2	15.6	20.9	32.0	J	12.8	18.7	30.2
J3	12.7	18.3	34.5	Avg	12.2	19.0	36.3
J4	14.3	20.8	31.9				

tire vertical load is found to be insignificant on the duration of τ_1, τ_2, or τ_3 (Table 6) for each of the three surfaces. In fact, the average transient-time duration τ_1 or τ_2 for the three test series is approximately the same, which suggests that the effect of texture is also insignificant on the transient-time duration. Thus it can be concluded that the transient-time durations are independent of the changes in the operating parameters. Similar conclusions were also drawn from the laboratory tests on the fine-textured belt. As in the laboratory tests, the final BFC values (steady-state BFC) decrease with increasing speed. This trend, which has been well documented (6,8), supports the experimental procedure and also, in turn, supports the validity of the laboratory tests. It may be recalled that similar trends were noted in the laboratory test results also.

COMPARISON OF LABORATORY AND HIGHWAY TEST RESULTS

Figure 8 shows a comparison of typical friction-time traces from the laboratory tests and the highway tests. Although the test conditions are different, the traces are similar in qualitative shape. Moreover, the transient-time durations under these different operating conditions are also similar (16.5 ms in the laboratory versus 17.6 ms on the highway).

The similarity between the highway tests and the laboratory tests establishes the following facts:

1. The laboratory test results represent realistic highway situations as far as the character of the transient time from the nonhydroplaning state to the hydroplaning state is concerned and
2. The character of the transient time is unaffected by operating parameters (speed, film thickness, inflation pressure, or texture).

The duration of the transient condition during which the available friction value decreases varies between 7 and 65 ms under a broad spectrum of operating conditions. For practical purposes, this response-time range is instantaneous when compared with other response times in the complete system of vehicle and driver. Driver response is of the order of 1-2 s and the vehicle-response times are of the

Figure 8. Comparison of laboratory test on textured belt with highway test on Jennite.

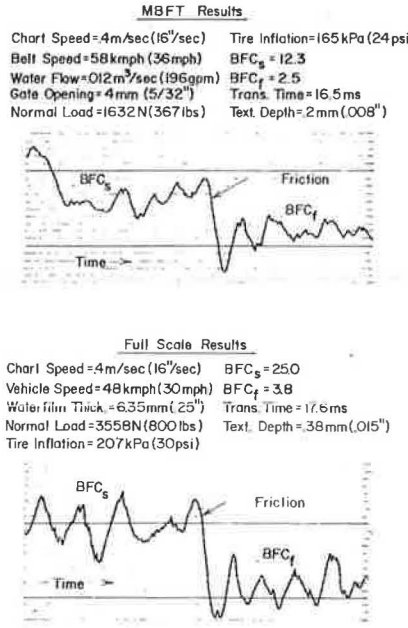

order of 1-1.5 s. These are an order of magnitude greater than the tire-response times found in this study. The significance of this finding is that, for a simulation of a vehicle, the tire characteristics can be considered instantaneous when conditions such as the water-film thickness change instantly.

CONCLUSIONS

The following conclusions are drawn from the results of this research:

1. When a moving tire encounters a sudden increase in the water layer in its path, up to 65 ms are required for the friction force to drop from a nonhydroplaning condition to a hydroplaning condition in the region of the thick water layer. Speeds during this transitory period range from 48 to 96 km/h (30-60 miles/h).
2. The laboratory and the highway tests show that, in the range of operating variables considered, the transient times do not vary significantly. These times can be considered instantaneous when compared with the complete system of vehicle and driver. Thus highway-maintenance requirements are dictated by the vehicle response to these transient inputs.
3. The friction force goes through a minimum value before reaching the steady state. However, the time during which the friction force is below the steady-state value is very short.

It is suggested that further study of tire hydroplaning during sudden changes in the water layer in the path of the tire would be worthwhile. Specifically, the following recommendations are made:

1. Since the mechanics of tire-contact-area deformation are different for a radial tire than for bias and belted tires, transient and steady-state hydroplaning characteristics of radial tires should be investigated.
2. The effect of the transitory period on the vehicle dynamics characteristics should be studied. This may clarify some of the problems associated with differential braking of vehicles that result in loss of directional control.

ACKNOWLEDGMENT

This research was sponsored by the Office of University Research of the U.S. Department of Transportation. The progress of the research was aided by valuable suggestions from R. R. Hegmon, contract monitor, and from W. E. Meyer, professor emeritus of mechanical engineering, Pennsylvania State University. The opinions, findings, and conclusions expressed in this paper are ours and not necessarily those of the sponsor.

REFERENCES

1. W. B. Horne and U. T. Joyner. Some Effects of Runway Slush and Water on the Operation of Airplanes, with Particular Reference to Jet Transport. Presented at International Congress of SAE, Detroit, MI, Jan. 11-15, 1965, SEA Paper 970C.
2. S. K. Agrawal, W. E. Meyer, and J. J. Henry. Measurement of Hydroplaning Potential. Pennsylvania State Univ., University Park, Rept. PTI 7701, Feb. 1977.
3. A. L. Browne. Dynamic Hydroplaning of Tires. Northwestern Univ., Evanston, IL, Ph.D. dissertation, 1971.
4. H. Daughaday and C. Tung. A Mathematical Analysis of Hydroplaning Phenomena. Cornell Aeronautical Laboratory, Buffalo, NY, Rept. AG-2495-5-1, Jan. 1969.
5. S. K. Agrawal. Transient Aspect of Hydroplaning: Hydroplaning Phenomena During Sudden Changes in the Fluid Layer on a Pavement. Department of Mechanical Engineering, Pennsylvania State Univ., University Park, Ph.D. dissertation, May 1979.
6. S. K. Agrawal and J. J. Henry. Technique for Evaluating Hydroplaning Potential of Pavements. TRB, Transportation Research Record 633, 1977, pp. 1-7.
7. J. D. Decker. The Improved Penn State Friction Tester. Automotive Research Program, Pennsylvania State Univ., University Park, Rept. S58, Dec. 1973.
8. W. B. Horne and R. C. Dreher. Phenomena of Pneumatic Hydroplaning. National Aeronautics and Space Administration, Tech. Note TN D-2046, Nov. 1963.

Effects of Pavement Contaminants on Skid Resistance

ROGER B. SHAKELY, JOHN JEWETT HENRY, AND ROBERT J. HEINSOHN

It is known from previous research that skid resistance can vary significantly on a daily basis. The cause of this short-term variation may be attributed to external factors such as amount and intensity of rainfall and contamination effects of debris on the road surface. For this study, daily skid-resistance measurements were taken on the road surface according to ASTM E274-77 and a sample of dust and debris was collected from the road surface and analyzed for size distribution. It was found that the major factor that influenced the short-term skid resistance was dust particles in a certain range of sizes found on the road.

Road-surface friction characteristics vary throughout the year due to factors such as pavement polishing or wear, amount of precipitation, and road-surface contamination (1). Each of these factors separately plays an important part in determining the skid resistance of a road surface, but there is also a strong interaction among them that affects pavement friction characteristics.

Pavement polishing increases with traffic density for a given pavement. Polishing alone will lower skid resistance of pavements due to the overall effect of wearing down of the pavement texture. The grinding action between the tire and the road surface creates a very fine abrasive compound made up of tire and road-surface compounds together with ground-up particles of wind-blown soil and debris. These particles may adhere to tires, become airborne as fugitive dust emissions, or remain on the road surface. The particles that remain on the road and in the tire path affect the skid resistance by filling in some of the small asperities. The small asperities that are smaller than 500 μm are defined as the pavement microtexture; those larger than 500 μm are defined as the macrotexture (2). The greater the particle loading in the tire path, the lower the skid resistance at low tire slip speeds. The size of these particles is in the microtexture range of the pavement and they provide a crude form of lubrication on the road surface by preventing good contact between the tire and the pavement at the microtexture level. This is an important factor in skid resistance at tire slip speeds less than 16 km/h (10 miles/h).

The effect of rain on pavement skid resistance has received more attention than the effect of contaminants. The amount of water between the tire and the pavement and how easily it is channeled away has a very significant effect on skid resistance. The action of channeling the water from the tire-pavement contact will produce a cleansing effect on the road surface. This cleansing effect, which washes away the fine aggregate created by the road polishing, will increase the skid resistance of the road surface. It also provides for maximum contact between the tire and actual pavement surface and results in a maximum skid resistance for the road surface.

The objective of this research is to study the effect that unbonded material that lies on the road surface has on the short-term variation of skid resistance and polishing. This research included the design and construction of a device that can be mounted on a moving vehicle that is traveling at a speed of 16 km/h and can remove, collect, and separate according to size unbonded material on the road surface.

SKID-RESISTANCE MEASUREMENTS

The skid resistance of the pavement tested in this study was measured in accordance with ASTM E274-77. This method of test measures the friction force of a vertically loaded test tire that is sliding over the pavement at a constant velocity. The immediate results are expressed as locked-wheel skid numbers (SNs), defined as follows:

$$SN_v = [\text{locked-wheel friction force at velocity (v)/normal load}] \times 100 \quad (1)$$

A skidding velocity of v = 64 km/h (40 miles/h) is normally used for these tests, and the SN is expressed as SN_{40}. The microtexture of a pavement affects the skid resistance at low tire slip speeds (3). In order to obtain information about the microtexture, it would be necessary to run locked-wheel skid tests at very low speeds, which can create traffic hazards. The method chosen to obtain microtexture information for this study was to measure the skid resistance as the test tire was locked; the resulting slip range was 0 to 64 km/h. The transient portion of the tire lock-up contains the same skid data as would be obtained if separate locked-wheel skid tests were run at specific speeds between 0 and 64 km/h (3). Therefore, the SNs at 16, 32, 48, and 64 km/h were obtained from one transient slip test at 64 km/h. These data points are recorded in Table 1, and a statistical regression analysis was performed on each day of recorded data. The regression program computed a least-squares fit of the four pairs of data points (SN and slip speed) to an exponential function of the following form:

$$SN_v = SN_0 \exp(bV) \quad (2)$$

where

SN_v = SN at slip speed v,
SN_0 = SN intercept determined by the regression analysis,
b = -PNG/100 percent SN gradient determined by the regression analysis (PNG = percentage of normalized gradient), and
V = slip speed of the test tire.

This is the Pennsylvania State University model (2) for skid resistance; it is used here to determine SN_0, the SN intercept. SN_0 characterizes the skid resistance at low speeds. The correlation coefficient for this curve fit was consistently more than 95 percent. From these results, SN_0 was used to represent the condition of the microtexture of the pavement.

EFFECT OF CONTAMINANTS ON ROAD SURFACE

Contamination of the road surface does have a major effect on skid resistance. The dust and debris that have settled on the pavement change the microtexture by filling the small asperities and thus affect the tire-pavement interaction. The type of contaminants in this size range (known as traffic or surface film) include dust, sand, oil, grease, organic debris, rubber particles, mud, and chemical treatments. All these will affect the condition of the microtexture. A case in point, which further

Table 1. Transient skid-resistance data.

Date	SN_0	SN_{16}	SN_{32}	SN_{48}	SN_{64}	PNG	R^2 (%)
9-21-77	58.7	51.5	45.5	41.0	35.0	1.26	99
9-29-77	53.2	48.6	39.5	35.5	33.0	1.27	97
9-30-77	58.8	51.5	43.0	35.5	33.0	1.53	98
10-3-77	58.5	52.0	43.0	37.0	34.0	1.42	99
10-4-77	53.6	48.0	38.0	34.0	30.5	1.47	98
10-5-77	54.6	48.5	42.5	38.0	33.5	1.22	99
10-7-77	58.6	51.5	46.0	42.0	35.5	1.21	99
10-10-77	53.2	47.0	43.0	39.5	33.5	1.10	99
10-11-77	60.6	53.0	44.5	39.5	34.0	1.45	99
10-12-77	52.5	47.5	41.5	37.0	34.0	1.12	99
10-13-77	52.2	48.5	40.0	37.0	34.5	1.10	97
10-14-77	60.3	54.0	43.0	37.5	34.5	1.48	98
10-17-77	61.4	55.6	47.5	43.0	39.0	1.16	99
10-18-77	59.7	54.5	45.0	40.0	37.5	1.24	97
10-21-77	55.9	51.0	45.0	41.5	37.5	1.00	99
10-24-77	54.5	49.6	47.0	41.5	39.0	0.85	99
10-25-77	54.2	50.0	44.0	39.0	37.5	0.98	98
10-26-77	53.5	50.0	43.0	38.5	37.5	0.97	96
10-28-77	56.7	53.0	44.0	42.0	38.5	1.00	96
10-31-77	56.2	51.0	45.0	41.5	37.0	1.04	99
11-2-77	60.1	55.5	44.5	40.0	38.0	1.24	96
11-14-77	53.7	49.5	43.0	38.5	36.5	1.02	98

demonstrates the effect of debris on the road surface, was noted during the course of this study. Work crews were removing the painted lines on the road by grinding away the painted surface. This grinding action created large quantitites of small particles that spread over the road surface. Results of skid tests at this location gave lower results by 11 SNs compared with results from the rest of the sites on the same road.

The effect of rain observed in this study was to increase the skid resistance of pavements by removing all or portions of the contaminants on the road surface. Road contamination that results from traffic film can significantly reduce the SN of a pavement that has fine asperities only. For example, Kummer and Meyer reported a rise in the SN from 11 to 20 for tests made just before and after a rain preceded by a long dry period (4). Skid tests were made on concrete pavements after a 15.4-mm (0.6-in) rain that was preceded by 20 days with no measurable precipitation. The data showed that the SN_{40} values had increased by a greater percentage on pavements that had the lower values prior to the rain. In general, the SNs obtained after the rain increased from 6 to 18 percent; the 18 percent increase occurred on a pavement that had an initial value of 40 and the 6 percent increase was for pavement that had an initial value of 60 (5). If there is no heavy rainfall to cleanse the road surface, it can become slippery when slightly wet due to the lubricating slurry of the water and dust debris (6).

The amount and frequency of the rain has a great influence on the accumulation of the traffic film, since rain is instrumental in washing it away. Hence, the degree to which the traffic film lowers the antiskid properties of a pavement depends on the period between rainfalls. The shorter the period, the shorter the time the film has to significantly accumulate on the road surface (6).

Dust generation and hence aggregate polishing are caused by tires rolling over the pavement. Motion takes place between the tread rubber and pavement as the tire deforms in the contact patch. In the presence of particles, this leads to the wear and polishing of the pavement. The pavement (particularly exposed aggregate) may become smoother or rougher than it was before, depending on the size and characteristics of the particles. The dust on the road most frequently originates from the pavement itself but may also be blown in from the shoulders or elsewhere.

ROAD VACUUM DEVICE

The design considerations for a vehicle-mounted road-dust collection device were as follows:

1. The vacuum system must be able to pick up unbonded road dust and particles in the wheel track of the road;
2. The system must be mounted on the front of a moving vehicle in order to assure minimum disturbance of the dust in the wheel track, which would otherwise occur if the vehicle were to pass over it;
3. The transportation of the dust particles must be for as short a distance as possible and with a minimum number of turns to reduce settling and impaction;
4. The method of particle collection should enable a quick and accurate analysis of the size distribution of the dust (otherwise the determination of particle size and distribution would have to be performed optically and would consume a considerable amount of time).

These design parameters were considered in the construction of the system shown in Figures 1 and 2.

The dust collector is attached to the front bumper of the Pennsylvania Transportation Institute (PTI) Mark 3 pavement skid tester. A beam hinged at the truck bumper extends down toward the pavement and attaches rigidly to a carriage mechanism. A two-wheeled carriage is used to support the vacuum hood in order to allow the hood to follow the road surface with much greater accuracy than would a system rigidly mounted on the truck. The front of the vacuum hood is attached to the carriage by a system of hinges and the back is supported by a cable that extends down from the beam. The hinges on the front of the hood and the cable in the rear allow the hood to swing up and back in order to prevent damage to the system if it comes in contact with a large stone or other obstacle on the road.

Suction at the hood is provided by a fan connected to the back of the Anderson 2000 high-volume cascade impactor, which serves as the filtration and separation system. The volumetric air-flow rate through the system is regulated by adjusting a Variac connected to the fan. The flow rate is read in the truck by using a rotameter designed for use with the cascade impactor.

The power for the fan is supplied by a 120-V AC generator carried in the back of the truck bed. Compressed air used in the operation of the vacuum hood is supplied by a compressor, which fills a supply tank in the front of the truck. The compressed air is used to aid in the dislodging of particles from the road surface by incorporating an air knife into the design of the hood.

The dust collection was carried out on a daily basis (weather permitting) between September 24 and November 14, 1977. The collections were made in the early afternoon on the same inside wheel track on a 545-m (1800-ft) section of dense-graded asphalt concrete pavement that contained limestone coarse aggregate. By collecting dust at two skid sites daily, the average road dust and skid resistance for the section of road was determined.

EXPERIMENTAL RESULTS AND INTERPRETATION

Location of Test Site

The location of the 545-m test site was a rural

road. The dust accumulation on it should be representative of that generated solely by traffic. The area that surrounded the test section was covered with vegetation, and there was little exposed soil that could be blown onto the road by wind erosion. The amount of road dust collected is given in Table 2. Figure 3 gives the rainfall and skid-resistance data that were recorded from April 20 through December 1, 1977. Road-dust collection was carried out between September 24 and November 24, 1977. The average daily traffic count on PA-45 during this time was 775 cars.

Figure 1. Skid tester and dust-collection system.

Figure 2. Dust-collection system.

Correlation Between Road Dust and Skid Resistance

The pavement friction of the test site varied on a daily basis. The reason for this variation can be explained to some degree by the quantity of dust in the tire path. The values used to represent the pavement skid resistance are the SN_0 values, which characterize the skid resistance at low speeds. SN_0 is an indicator of the condition of the microtexture of the pavement, since the low-speed skid resistance is dependent on the microtexture of the pavement (2). The mass mean diameter of all the particles collected, except those in the preseparator (which collected particles larger than 50 μm) is 5 μm. This would affect the microtexture of the pavement (asperities smaller than 500 μm) more than the macrotexture (asperities larger than 500 μm).

Dust loading of the sample that contained particles 7.0-50.0 μm in size and SN_0 versus the date of collection is illustrated in Figure 4. This plot gives an indication of the interaction between the dust on the road and skid resistance on a daily basis. This interaction is an inverse relationship between the amount of dust and the SN. A linear regression analysis was conducted to determine the correlation between the amount of dust in the wheel track and the skid resistance. Different combinations of dust size and quantity were regressed against the SN_0 value for each day. The particles collected in the preseparator were not included in the analysis because of their large size and small amount. Table 3 gives the results of this analysis.

The highest correlation between road dust and skid resistance was found for particles in the size range 7.0-50.0 μm. The linear regression equation that relates SN_0 to grams per square meter of the dust sample of 7.0-50.0 μm from the test section is as follows:

$$SN_0 = 60.99 - 951.0M1 \quad (3)$$

where M1 is the dust loading in grams per square meter of the 7.0- to 50.0-μm dust sample collected at the test site. This equation results in a correlation coefficient of 60.1 percent.

Table 2. Mass loading per square meter for various sizes of dust particles collected along test section.

	Mass Loading (mg/m^2) by Particle Size					
Date	Larger than 50 μm	7.0-50.0 μm	3.3-7.0 μm	2.0-3.3 μm	1.1-2.0 μm	Smaller than 1.1 μm
9-21-77	0.00	3.11	1.07	0.987	0.251	0.746
9-29-77	0.00	5.27	1.77	1.22	0.248	2.190
9-30-77	0.00	4.13	2.01	1.20	0.377	1.260
10-3-77	9.69	3.63	1.17	0.890	0.240	0.990
10-4-77	18.60	5.01	1.72	0.908	0.309	1.550
10-5-77	11.20	4.38	1.29	0.807	0.262	0.983
10-7-77	18.80	3.73	1.19	0.753	0.208	1.050
10-10-77	55.40	6.80	1.66	1.380	0.344	1.480
10-11-77	17.60	1.75	8.79	0.513	0.118	0.563
10-12-77	53.10	6.48	1.92	0.954	0.330	1.350
10-13-77	25.00	5.51	1.88	1.190	0.488	1.030
10-14-77	6.75	2.38	9.66	0.786	0.319	0.398
10-17-77	11.50	1.79	1.14	0.585	0.258	0.879
10-18-77	16.20	1.84	1.07	0.653	0.488	0.825
10-21-77	21.60	4.52	5.42	1.190	0.366	1.170
10-24-77	36.40	8.56	2.97	1.880	1.170	2.090
10-25-77	28.10	9.10	2.88	1.790	0.535	1.850
10-26-77	17.40	7.65	2.63	1.630	0.380	1.140
10-28-77	8.93	2.95	1.14	0.657	0.240	0.474
10-31-77	7.00	3.90	1.76	0.807	0.337	0.527
11-2-77	7.57	3.24	7.82	0.470	0.097	0.377
11-14-77	16.90	10.60	3.26	1.730	0.484	1.830

Figure 3. SN_0 for PA-45 and University Drive versus date and rainfall.

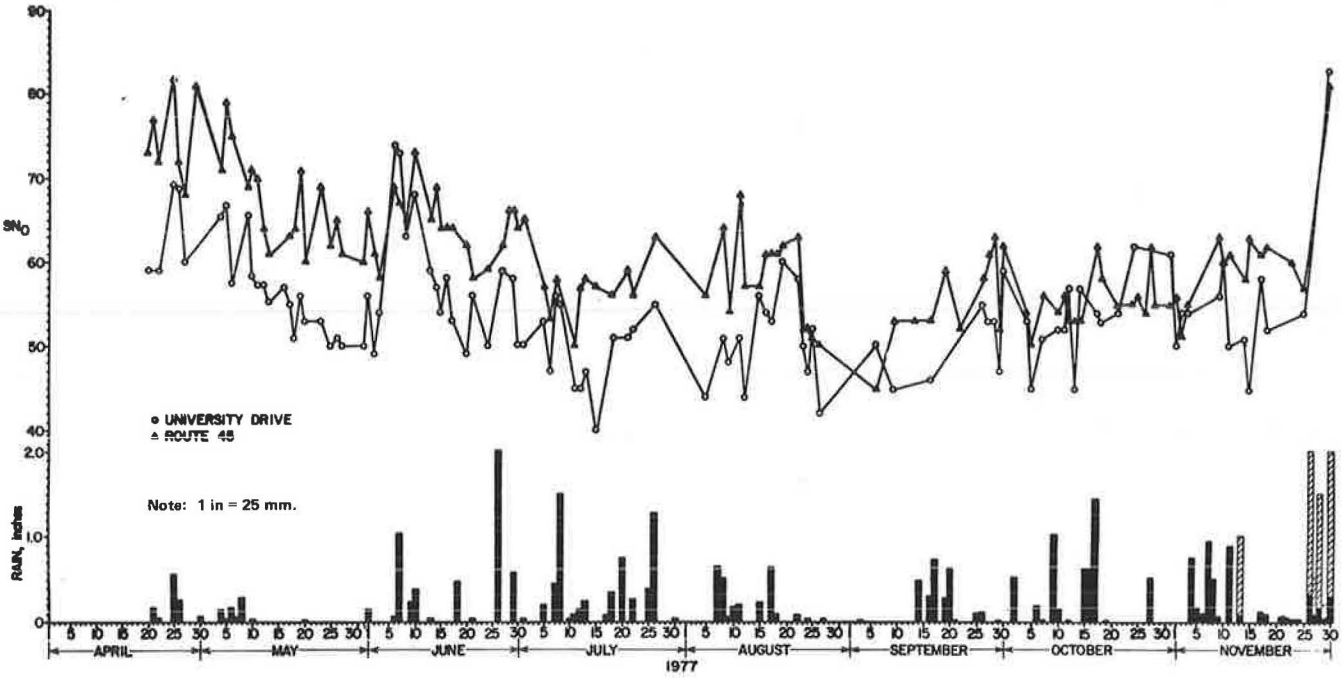

Figure 4. Dust loading of dust sample 7.0-50.0 μm and SN_0 versus date of collection.

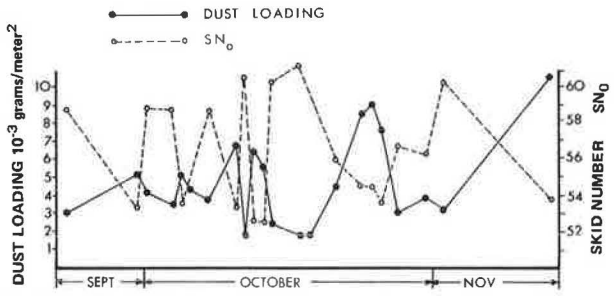

Figure 5. SN_0 versus dust loading of dust samples 7.0-50.0 μm.

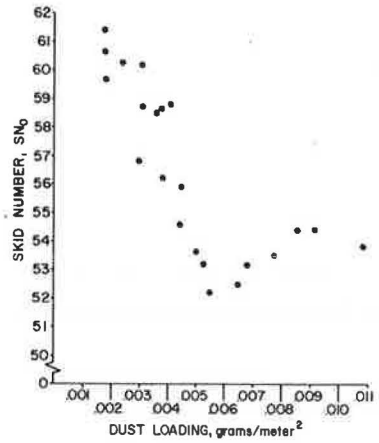

Table 3. Regression analysis to determine relationship between daily dust samples and SN_0.

Sample	Regression Equation	R^2 (%)
M1 (7.0 - 50.0 μm)	$SN_0 = 60.99 - 951.0M$	60.1
M2 (3.3 - 7.0 μm)	$SN_0 = 61.24 - 2877.0M$	46.4
M3 (2.0 - 3.3 μm)	$SN_0 = 61.39 - 4784.0M$	44.2
M4 (1.1 - 2.0 μm)	$SN_0 = 58.29 - 5320.0M$	44.3
M5 (< 1.1 μm)	$SN_0 = 60.66 - 3793.0M$	44.8
M1 + M2 + M3 + M4 + M5	$SN_0 = 61.45 - 558.0M$	57.6
M1 + M2 + M3 + M4	$SN_0 = 61.29 - 619.0M$	56.4
M1 + M2 + M3	$SN_0 = 61.30 - 649.0M$	57.4
M1 + M2	$SN_0 = 61.18 - 735.0M$	58.2

Notes: 1 km/h = 0.6 mile/h.
SN_0 = SN at 0 km/h as determined by an exponential curve fit to a transient SN analysis.
M = dust loading in grams per square meter of dust collected in a particular size range.

A plot of SN_0 versus the loading of the dust sample of 7.0- to 50.0-µm collected between September and November is shown in Figure 5. It is interesting to note the maximum loadings of dust collected on the test section, which are in the range of 0.007-0.011 g/m². In this range, the straight-line relationship changes for loadings greater than 0.007 g/m². This could be due to an effective saturation of the microtexture by the dust. That is, increased dust loadings may have no significant effect on the SN_0 values of the pavement. Examination of the SN_0 data from August through November indicates that only once did the SN_0 value for the test site drop below 50. This may indicate that other factors that limit SN_0 begin to take effect and dust loading loses its effect.

A regression analysis performed on the loadings of dust collected in the 7.0- to 50.0-µm range (leaving out the four points whose loadings are larger than 0.007 g/m²) results in an equation that fits the remaining data with an 82 percent correlation coefficient:

$$SN_0 = 64.21 - 1862.0M1 \quad (4)$$

From this study and a review of the 1977 SN_0

Table 4. BPN values from pavement before and after cleaning.

Location	Test No.	BPN Values: Contaminated Pavement Trial 1	Trial 2	Trial 3	Avg	Cleaned Pavement Trial 1	Trial 2	Trial 3	Avg
Asphalt parking lot	1	83	83	83	83.0	86	87	86	86.3
	2	69	69	69	69.0	73	72	72	72.3
	3	69	67	67	67.7	70	72	70	70.7
Avg					73.2				76.43
PA-45	1	57	57	57	57.0	61	60	60	60.3
	2	60	61	61	60.7	65	64	62	63.7
	3	67	67	68	67.3	75	74	74	74.3
	4	71	71	70	70.6	76	78	76	76.7
	5	61	61	60	60.6	67	67	66	66.7
	6	64	63	63	63.3	65	66	65	65.3
Avg					63.3				67.8

Figure 6. BPN values from surfaces before and after cleaning.

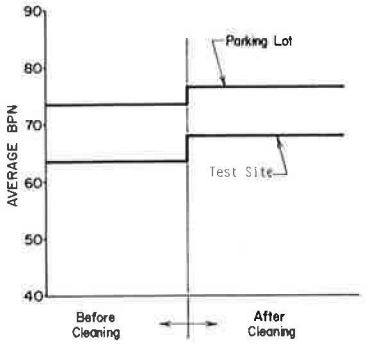

Figure 7. SN_{17} from contaminated and cleaned section of the test site.

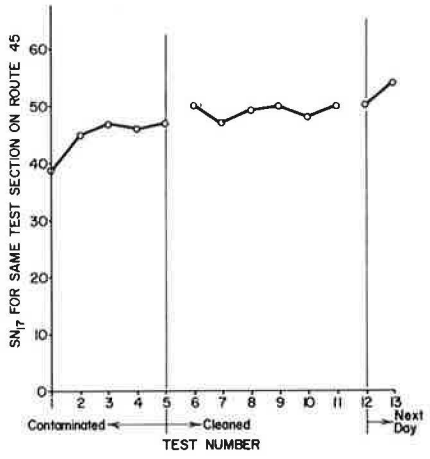

data in Table 1, it appears that a dust loading greater than 0.007 g/m² will result in no further effect on the SN_0 value for the test section.

Verification of Interaction Between Dust and Low-Speed Skid Resistance

It has been postulated that one cause of daily variation of skid resistance at low speeds is the changing contamination levels on the road surface. An attempt was made to verify this by conducting a series of tests to specifically verify interaction between low-speed skid resistance and dust loading on a pavement surface.

The first of these tests used a British pendulum tester, which measures the low-speed skid resistance. The procedure followed the one specified in ASTM E303 except that the pavement surface was not cleaned for the first portion of the test. British pendulum tests were run on the contaminated pavement and the British-pendulum-number (BPN) values for the three trials were recorded. Next, the same location on the pavement was scrubbed to remove the contaminants, and the BPN values for the three trials were recorded. The results of these tests indicated an average rise in the BPN values of 3.2 for the three tests in the asphalt parking lot and an average increase of 4.5 in BPN values for the six tests taken on PA-45. BPN values before and after cleaning are shown in Figure 6 and Table 4. Both groups of tests show a significant and consistant increase in the low-speed skid resistance of the surfaces.

A second test was run at the test site with the PTI Mark 3 skid tester. A series of five skid tests was run at the same location at the test site at a speed of 27 km/h (17 miles/h). After these five skid tests, that section of pavement was scrubbed three times by using water and a stiff broom in order to remove the contaminants in the wheel track. Six more 27-km/h skid tests were run on the cleaned section of road to check for any change in skid resistance. Two more 27-km/h skid tests were run the next morning after a heavy rain that occurred the evening of the day the road was scrubbed.

The results of this test also indicate a significant rise in SN_{17}. An average rise in SN_{17} of 2.8 resulted in the data taken before and after scrubbing. A plot of SN_{17} on pavement before and after it was scrubbed is shown in Figure 7. SN_{17} is a less-sensitive indicator of low-speed skid resistance than SN_0, but it clearly indicates that the cleaning of dirt from the wheel track will result in increasing the track's low-speed skid resistance.

CONCLUSIONS

The skid resistance of a surface will vary due to many factors. These include the type of surface being tested, the contaminants on the surface, and the speed at which the test takes place. This study was limited to one road surface. It resulted in a straight-line relationship between SN_0 and dust loading up to a point at which it appears that the further increase in dust loading has no further effect on the reduction of the SN_0 values.

That dust has an effect on low-speed skid resistance was proved by the British pendulum tests made on several contaminated and cleaned surfaces.

Skid tests on contaminated and cleaned sections of pavement also verified these results.

Particles smaller than 7 μm appear to have no significant effect on the SN_0 values for the surfaces used in this study. A collection system that separates particles out in stages from 10 μm to 500 μm would be more useful in determining relationships between SN_0 and dust loadings.

REFERENCES

1. J. M. Rice. Seasonal Variation in Pavement Skid Resistance. Public Roads, Vol. 40, March 1977.
2. M. C. Leu. The Relationship Between Skidding Resistance and Pavement Texture. Pennsylvania State Univ., University Park, Automotive Res. Program Rept. S78, 1977.
3. V. Shah. Relationship of Locked-Wheel Friction to That of Other Test Modes. Pennsylvania State Univ., University Park, Pennsylvania Department of Transportation Project 72-7, Final Rept., 1977.
4. H. W. Kummer and W. E. Meyer. Rubber and Tire Friction. Department of Mechanical Engineering, Pennsylvania State Univ., Automotive Safety Project, Engineering Res. Bull. B-80, 1960.
5. B. E. Colley, A. P. Christensen, and W. V. Nowlen. Factors Affecting Skid Resistance and Safety of Concrete Pavements. HRB, Special Rept. 101, 1969.
6. K. C. Ludema. An Analysis of the Literature on Tire-Road Skid Resistance. Mechanical Engineering Department, Univ. of Michigan, Ann Arbor, 1973.

Recent Developments in Pavement Texture Research

G. G. BALMER AND R. R. HEGMON

This paper summarizes the state of the art of research on pavement texture, which has intensified during the last few years. The importance of texture for increased safety on wet roads has been established. The distinct contributions of microtexture and macrotexture to friction between tire and pavement are shown, and methods being developed for providing and maintaining adequate texture are discussed. Research now in progress both on improving methods of texture measurement and on developing models for predicting skid resistance and gradients of skid resistance and speed from texture measurements is described.

Effective pavement texture is essential for safer wet-weather highway travel. The fine features (microtexture) furnish a gritty surface to penetrate the thin water films and produce skid resistance through good adhesion between the tire and pavement surfaces. The coarse features (macrotexture) provide drainage channels for water expulsion between the tire and the roadway. This allows better tire contact with the pavement to improve skid resistance and mitigate hydroplaning (1,2). It yields a flatter gradient of wet-pavement skid resistance and speed that helps sustain good friction for high-speed traffic, because the water can escape faster through a coarser texture. A knobby or coarse-textured surface also causes larger rubber deformations, which result in hysteresis losses in the tire. These increase the tire friction characteristics.

Furthermore, it has been shown that the wet-pavement accident rate decreases as skid resistance increases (3). Thus, effective pavement texture is an important factor in traffic safety.

TEXTURE CLASSES AND FUNCTIONS

The fine features of a pavement surface are distinguished from the coarse features because of the different influences of these parameters on interactions between tire and pavement.

The microtexture contributes to skid resistance at all speeds, and it is the prevailing influence at speeds less than 50 km/h (31 miles/h). In contrast, the macrotexture is less important at low speeds, but a coarse macrotexture is essential for safer high-speed travel on wet pavements. Average texture depths of 0.5 mm (0.02 in) and less can be classified as microtexture and those larger as macrotexture.

TEXTURE CHARACTERISTICS

The pavement microtexture develops skid resistance through adhesion between the tire and the roadway. The sharp, fine particles (asperities) in the surface penetrate the thin water films and thus permit an intimate contact between the tire and the roadway. Microtexture depends largely on the mineral composition and the rugosity of the aggregates. The fine, hard grains in the coarse aggregates or fine aggregates bonded in the surface of the pavement provide the microtexture.

Ideally, aggregates for bituminous concrete should be composed of hard, coarse, angular minerals well bonded into a softer matrix so that gradual differential wear will occur (4).

Pavement macrotexture can be obtained by controlling the gradation (5,6) of the surface aggregates in a bituminous mixture such as the open-graded asphalt friction course. The surface aggregates must not polish readily if enduring skid resistance is to be maintained. Figure 1 (from the Texas Transportation Institute) is a photograph of a newly placed open-graded asphalt friction course. The coarse texture is visible in the foreground. Chip-seal surface treatments also produce a coarse macrotexture; however, these surfaces have a limited life because of the rapid erosion of the surface aggregates by traffic and weathering.

The macrotexture for portland cement concrete (PCC) pavement is produced by the finishing techniques (1). Excellent texture can be obtained by using steel tines (Figure 2). (Figures 2-4 are from experimentation by the Georgia State Department of Transportation.) In this photograph alternate tines have been bent upward to increase the spacing between tines. Steel tines (rakes or combs, as they are sometimes called) can be incorporated into the paving train to produce striations in the plastic

Figure 1. Open-graded asphalt friction course.

Figure 2. Steel tines.

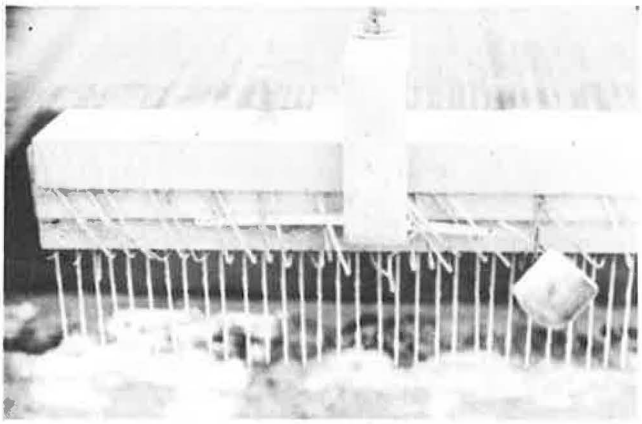

Figure 3. Typical tine-finished surface.

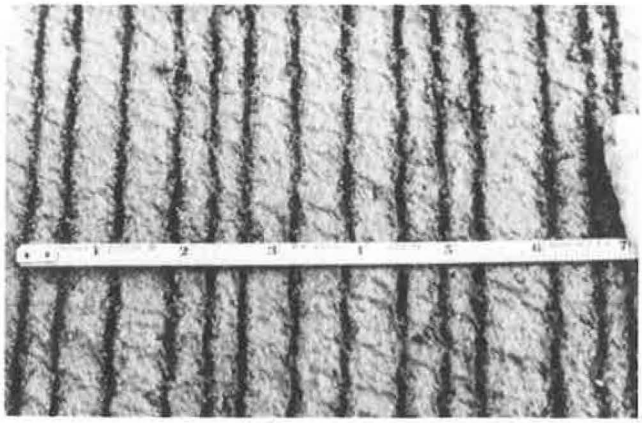

Figure 4. Gradient curves.

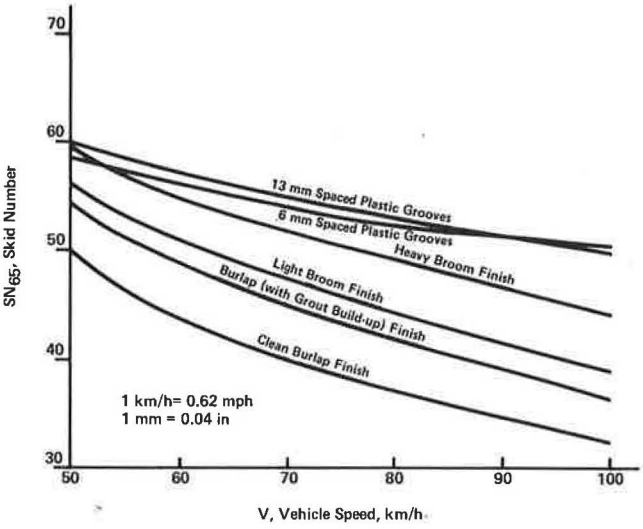

concrete. Figure 3 shows a typical tine-finished surface. The vibrating float developed in England (7) will also provide deep channels for surface water drainage. In the past, coarse brooms have been used for finishing PCC pavements, but such textures are usually not so good as the tine-finished textures.

In the photointerpretation method, developed by Schonfeld (6), texture is described by six parameters that are visually determined from sets of stereophotographs; for macrotexture of projections, the parameters are (a) height, (b) width, (c) angularity, and (d) density; for microtexture, they are (e) harshness, and (f) background harshness. A guide for the application of this method has recently been published (8).

GRADIENT

It is well known that the wet-pavement skid resistance decreases as vehicle speed increases (Figure 4). This is because the water has less time to escape from the contact areas between the tire and the road as the speed increases. Note that the skid numbers (SNs) are larger and the slopes flatter for the deep-finished surfaces (which have more space for water expulsion) than for the shallow-finished pavements. The former are the tine-finished surfaces labeled "spaced plastic grooves" in Figure 4.

Because of the wet-pavement surface, the friction-speed curve has a negative slope or a positive gradient as defined in the following equation:

$$G = -[d(SN)/dV] \quad (1)$$

where G is the gradient of skid resistance and speed and [d(SN)/dV] is the derivative of the SN with respect to vehicle speed (V) or the slope of the friction-speed curve at speed V. The gradient is greatly dependent on the macrotexture. A coarse macrotexture yields a flatter or better gradient.

Skid-resistance tests at one speed can be used to approximate the skid number (SN_V) for another speed (V), provided the gradient is known or can be determined. If one of the test speeds is 65 km/h (40 miles/h), SN_V can be computed from

Table 1. Values of SN_{65} computed from texture parameters.

	D (mm)							
BPN	0.5	1.0	1.5	2.0	2.5	3.0	3.5	4.0
30	7	8	8	8	9	9	9	9
40	16	18	19	20	20	20	21	21
50	25	28	30	31	32	32	33	33
60	34	39	41	42	43	44	44	45
70	44	49	52	53	55	55	56	57
80	53	59	63	65	66	67	68	69
90	62	70	74	76	78	79	80	81

$$SN_V = SN_{65} - (V - 65)G \quad (2)$$

Equation 2 can be generalized to determine the skid resistance from other test speeds. The accuracy of prediction decreases as the speed difference increases, because gradients are dependent on speed.

GRADIENT OF PERCENT-NORMALIZED SKID RESISTANCE AND SPEED

Research (4,9,10) has shown that the gradient not only is a function of macrotexture, but it also depends on the level of skid resistance. This led to the concept of the gradient of percent-normalized skid resistance and speed (PNG_V), defined for a particular speed (V) as

$$PNG_V = -(100/SN_V)[d(SN)/dV]_V \quad (3)$$

Equation 3 is the exact expression for the PNG, but it can be used only if an analytical relation between the SN and the speed has been established.

If the skid resistance is measured at two speeds (V_1 and V_2), PNG can be computed approximately from the following:

$$PNG_V = -\left\{100(SN_2 - SN_1)/[(V_2 - V_1)(SN_2 + SN_1)/2]\right\} \quad (4)$$

MODELS FOR FRICTION-SPEED CURVE AND PNG

Several models have been suggested to empirically represent the friction-speed curve. Leu and Henry (11) fitted the following exponential equation to skid-resistance speed data:

$$SN = p\exp(qV) \quad (5)$$

where p and q are constants, and exp is the base of natural logarithms. The constants in Equation 5 can be determined by as few as two points from the relationship between skid resistance and speed. If Equation 3 is applied to this model, it is found that

$$PNG = 100q \quad (6)$$

where q is a constant and thus independent of speed.

Other models have been proposed; however, none has been sufficiently validated.

MODEL FOR SKID RESISTANCE

The microtexture and macrotexture can be separated and combined in the model for skid resistance:

$$SN_V = SN_0 \exp[-(PNG/100)V] \quad (7)$$

where

SN_0 = intercept between SN and zero speed (a function of the microtexture),
PNG = percent-normalized gradient (a function of the macrotexture), and
V = speed selected for predicting SN_V.

A more-general form of the equation is

$$SN_V = SN_R \exp\left\{-[(PNG/100)(V - R)]\right\} \quad (8)$$

where R is any particular speed.

Skid tests (ASTM E274) and texture measurements (9,10) were conducted on 20 bituminous test pavements in West Virginia. Several techniques were used to measure pavement texture, and the data were analyzed from different approaches.

When British pendulum tests (ASTM E303) were conducted and a least-squares analysis was computed on the test data, the following equation was obtained:

$$SN_0 = 1.38BPN - 31 \quad (9)$$

where BPN is the British pendulum number.

One operator, from the West Virginia Department of Highways, conducted all the sandpatch (12) macrotexture measurements in order to obtain reliable results. The procedures were meticulous; therefore, consistency was achieved in the measurements.

An empirical model was introduced to express the relationship between PNG and the mean texture depth (D):

$$PNG = aD^c \quad (10)$$

The quantities a and c are constants.

An analysis of the data yielded

$$PNG = 0.73(D)^{-0.47} \quad (11)$$

where D is the sandpatch texture depth (mm).

When the test results of Equations 9 and 11 are substituted in Equation 7, and the velocity is converted to metric units, Equation 7 becomes

$$SN_V = (1.38BPN - 31)\exp[-0.0045V(D)^{-0.47}] \quad (12)$$

Numerical values may differ for data obtained from other sources, and they certainly will vary for different measurement techniques. Additional experimental measurements will help to stabilize the numerical values for Equation 7.

Equation 12 can be approximated by the following:

$$SN_{65} = (1.38BPN - 31)\exp[-(0.29/\sqrt{D})] \quad (13)$$

when V is 65 km/h (40 miles/h). The numerical values of Table 1 are computed from Equation 13.

RELATION OF TEXTURE PARAMETERS TO SKID RESISTANCE

The numerical values of Table 1 illustrate the effect of the texture parameters on the skid resistance. In the table, BPN represents the microtexture values; D represents the macrotexture. Table 1 shows that adequate microtexture is essential for good SNs, and the skid resistance increases as the microtexture increases.

SN also becomes larger as the macrotexture becomes larger, especially for large microtexture values. The dashed line separates values below and above an SN value of 40 for SN_{65}.

As examples, the table indicates that an SN value of 28 should be expected from a microtexture value of 50 and a macrotexture depth of 1 mm (0.04 in). A better value of 52 is to be expected from a microtexture value of 70 and a macrotexture depth of 1.5 mm (0.06 in).

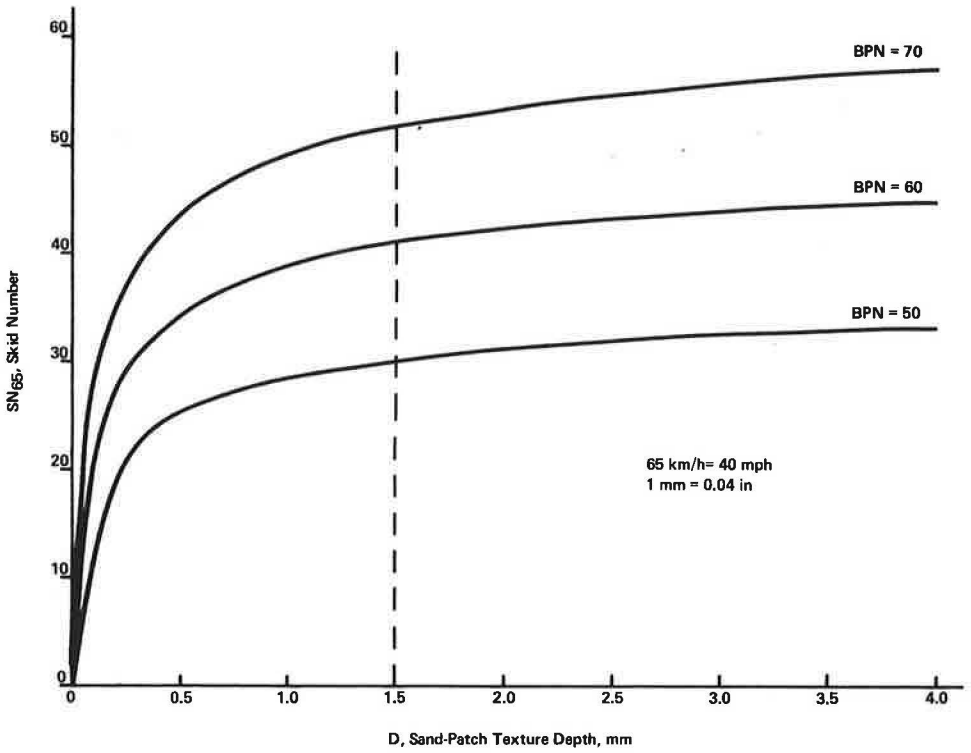

Figure 5. Effect of macrotexture on skid resistance.

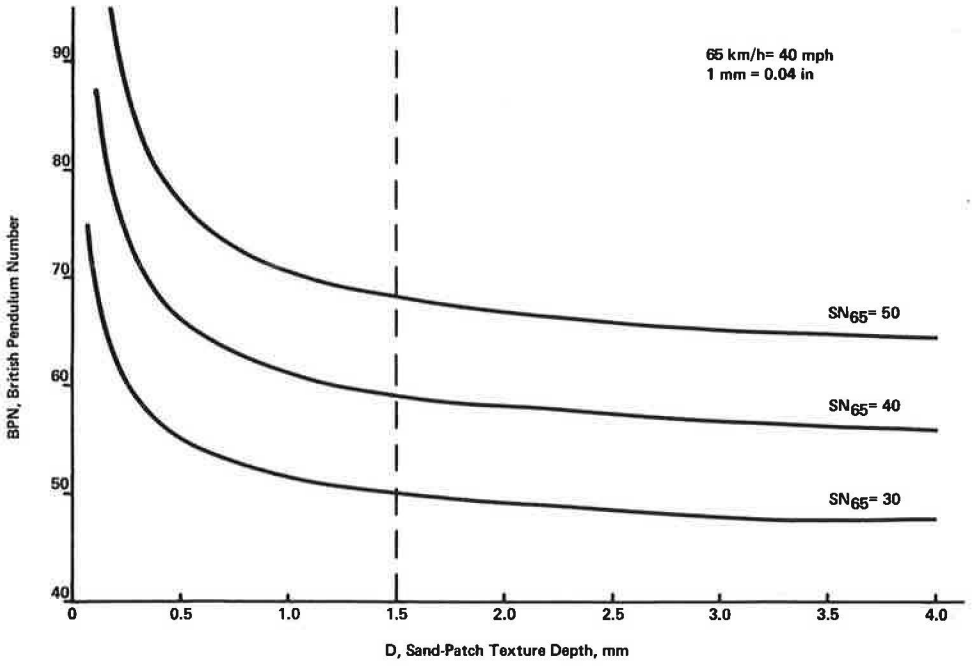

Figure 6. Texture requirements for specific skid resistance.

Similar tables can be calculated from Equation 12 for other speeds.

The influence of texture parameters on skid resistance is further illustrated in Figures 5 and 6. These curves are drawn from values computed from Equation 13. Relationships between two quantities can be shown graphically while a third quantity is held constant. Clearly, the SN in Figure 5 increases rapidly as the sandpatch texture depth increases to 1.5 mm for constant BPN values. Although the skid resistance increases above this value, the rate of change is smaller. A large value of microtexture is essential for adequate skid resistance when the macrotexture is small. This is illustrated in Figure 6.

Graphs can also be drawn to show the relationship between the microtexture and the SN for a constant macrotexture.

OTHER METHODS OF TEXTURE MEASUREMENT

The pavement microtexture can also be evaluated by locked-wheel skid tests at low speeds or by a microtexture profile tracer. The silicone putty impres-

sion test, the outflow meter, or a macrotexture tracer can be used to measure macrotexture. The profile tracer methods are limited mostly to laboratory use. If one or more of these methods are used, adjustments may be required in the texture numerical parameter values for the models.

ADDITIONAL RESEARCH

Research is being conducted to develop better texture-measurement techniques. Methods for both microtexture and macrotexture are under investigation.

Automated equipment in the laboratory (13) is being used to measure the aggregate shape factor (ratio of the average asperity height to the average width) for microtexture. The results from such measurements are correlating well with the polished stone value (PV) from the British wheel (ASTM D3319). The larger shape factors have larger polish values.

Research is also being conducted on macrotexture measurement at highway traffic speeds. It is directed toward a texture profile, a root-mean-square descriptor, or other similar descriptors, and it should relate to skid resistance, the gradient of skid resistance and speed, and the gradient of percentage of speed.

There is an implementation study in progress in which several states are evaluating the surface drainage measurement technique by means of the outflow meter.

FUTURE RESEARCH

There is a need for more research on pavement texture to determine its influence on noise generation, tire wear, pavement wear, and energy consumption. Other factors (4) to be considered are splash and spray, surface drainage during heavy precipitation, freeze-and-thaw behavior, night visibility, and snow-and-ice removal.

CONCLUSIONS

Skid resistance is determined and can be predicted for a selected vehicle speed from pavement-texture parameters. Empirical models provide a systematic basis for these predictions; however, the models cannot account for seasonal variations without supplemental information.

Adequate microtexture is essential for good skid resistance at all speeds and is the predominant factor for speeds less than 50 km/h (31 miles/h). Beneficial microtexture can be obtained from coarse aggregates that contain hard, angular, fine particles or harsh fine aggregates bonded in bituminous surfaces. Excellent microtexture is achieved for PCC pavements constructed by using hard, angular surface sands.

Coarse macrotexture is necessary for safe high-speed travel on wet pavements. It provides roadway surface voids to relieve the water pressure beneath the traveling tire. This reduces hydroplaning tendencies and increases the skid resistance because of better contact between tire and pavement.

Open-graded asphalt friction courses produce coarse macrotexture surfaces through mix design and selection of the proper aggregate sizes. Coarse macrotexture for PCC pavements can be obtained by deep tine finishes of the plastic concrete or by grooved hardened pavements.

Coarse-textured pavements finished by using steel tines develop larger SNs and smaller gradients than inferior-textured surfaces. The smaller gradients are especially important for better skid resistance at higher speeds.

Research and experience have shown that metal tines preceded by a burlap drag or other type of drag finish are practical and dependable means of providing excellent texture on PCC pavements.

The sample computations by using the texture and skid-resistance models show the interaction of both texture parameters for providing an adequate level of skid resistance. In particular, Table 1 and Figures 4-6 show that SNs increase significantly as the microtexture increases. It can be seen in Figure 5 that the skid resistance improves very rapidly as the macrotexture varies from 0 to 1.5 mm. Figure 6 shows that excellent microtexture is required to provide sufficient skid resistance when the macrotexture is small. The water-film thickness must also be thin enough for the microtexture to be effective; otherwise, there is a tendency for hydroplaning.

It appears that microtexture can be represented by measurements with the British pendulum tester. The macrotexture can be evaluated by the sandpatch or similar methods. There are also other techniques for measuring pavement texture, and research is continuing to appraise pavement surface characteristics at traffic speeds.

ACKNOWLEDGMENT

This is a condensation of a Federal Highway Administration ad hoc committee report. The report was presented informally to the Committee on Pavement Surface Properties and Vehicle Interaction during the 57th Annual Meeting of the Transportation Research Board.

1. G. G. Balmer. Pavement Texture: Its Significance and Development. TRB, Transportation Research Record 666, 1978, pp. 1-6.
2. B. M. Gallaway and others. Tentative Pavement and Geometric Design Criteria for Minimizing Hydroplaning. Federal Highway Administration, U.S. Department of Transportation, Rept. FHWA-RD-75-11, 1975, pp. 1-191. NTIS: PB 255748/AS.
3. R. L. Rizenbergs, J. L. Burchett, C. T. Napier, and J. A. Deacon. Accidents on Rural Interstate and Parkway Roads and Their Relation to Pavement Friction. TRB, Transportation Research Record 584, 1976, pp. 22-36.
4. S. H. Dahir and others. Alternatives for the Optimization of Aggregate and Pavement Properties Related to Friction and Wear Resistance. Federal Highway Administration, U.S. Department of Transportation, Rept. FHWA-RD-78-209, 1978, pp. 1-284.
5. R. W. Smith, J. M. Rice, and S. R. Spelman. Design of Open-Graded Asphalt Friction Courses. Federal Highway Administration, U.S. Department of Transportation, Rept. FHWA-RD-74-2, 1974, pp. 1-38. NTIS: PB 227479/AS.
6. R. Schonfeld. Photo-Interpretation of Pavement Skid Resistance in Practice. TRB, Transportation Research Record 523, 1974, pp. 65-75.
7. J. Weaver. Deep Grooving of Concrete Roads. Cement and Concrete Association, London, Oct. 1972; also presented at 2nd European Symposium on Concrete Roads (Bern, Switzerland, June 1973).
8. F. Holt and G. Musgrove. Skid Resistance: Photo-Interpreters' Manual. Ministry of Transportation and Communications, Downsview, Ontario, Canada, 1977.
9. W. E. Meyer, R. R. Hegmon, and T. D. Gillespie. Locked-Wheel Pavement Skid Tester Correlation and Calibration Techniques. NCHRP, Rept. 151, 1974, pp. 1-100.

10. E. D. Howerter, T. J. Rudd, and R. E. Sutermeister. Computer Evaluation of Pavement Texture. Federal Highway Administration, U.S. Department of Transportation, Tech. Rept. FHWA-RD-78-37, 1977, Vol. 2, pp. 1-100. NTIS: PB 293177/AS.
11. M. C. Leu and J. J. Henry. Prediction of Skid Resistance as a Function of Speed from Pavement Texture Measurements. TRB, Transportation Research Record 666, 1978, pp. 7-12.
12. M. C. Leu. Guidelines for Texturing of Portland Cement Concrete Highway Pavements. American Concrete Paving Association, Oak Brook, IL, Tech. Bull. 19, 1975, pp. 8-13.
13. S. W. Forster. Automated Aggregate Microtexture Measurement: Description and Procedures. Public Roads, Vol. 42, No. 3, Dec. 1978, pp. 99-104.